AD-A142 354 APPLICATION OF ADVANCED FRACTURE MECHANICS TECHNOLOGY TT ENSURE STRUCTURA..(U) WESTINGHOUSE RESEARCH AND DEVELOPMENT CENTER PITTSBURGH PA H A ERNST ET AL. 1/1

UNCLASSIFIED 22 NOV 82 82-9D7-TINAV-R1 N00014-80-C-0655 F/G 11/6 NL

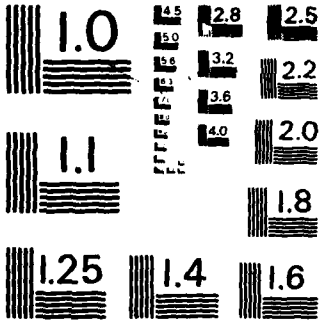

MICROCOPY RESOLUTION TEST CHART
NATIONAL BUREAU OF STANDARDS-1963-A

APPLICATION OF ADVANCED FRACTURE MECHANICS TECHNOLOGY TO ENSURE STRUCTURAL RELIABILITY IN CRITICAL TITANIUM STRUCTURES

H. A. Ernst and J. D. L[illegible]
Materials Engineering Department

NO DISTRIBUTION STATEMENT

WASHINGTON, DC 20375

AD-A142 354

November 1982

Contract No. N00014-80-C-0655

Final Report

Prepared for
OFFICE OF NAVAL RESEARCH
Department of the Navy
800 North Quincy Street
Arlington VA 22217

APPROVED FOR PUBLIC RELEASE
DISTRIBUTION UNLIMITED

DTIC FILE COPY

This document has been approved for public release and sale; its distribution is unlimited.

JUN 2 3 1984

[redacted] R&D Center
1310 Beulah Road
Pittsburgh, Pennsylvania 15235

84 06 18 207

APPLICATION OF ADVANCED FRACTURE MECHANICS TECHNOLOGY TO ENSURE STRUCTURAL RELIABILITY IN CRITICAL TITANIUM STRUCTURES

H. A. Ernst and J. D. Landes
Materials Engineering Department

November 1982

Contract No. N00014-80-C-0655

Final Report

Prepared for
OFFICE OF NAVAL RESEARCH
Department of the Navy
800 North Quincy Street
Arlington VA 22217

Westinghouse R&D Center
1310 Beulah Road
Pittsburgh, Pennsylvania 15235

82-9D7-TINAV-R1 November 22, 1982

APPLICATION OF ADVANCED FRACTURE MECHANICS TECHNOLOGY TO ENSURE STRUCTURAL RELIABILITY IN CRITICAL TITANIUM STRUCTURES

H. A. Ernst and J. D. Landes
Materials Engineering Department

ABSTRACT

This final report describes the work done in a program designed to assist the Navy in developing and applying fracture mechanics technology to assess structural reliability in critical applications of titanium alloys. A complete elastic-plastic fracture mechanics methodology is developed, and is applied to example models. Topics where further research is needed are discussed in detail.

DTIC COPY INSPECTED 2

A1

TABLE OF CONTENTS

1. INTRODUCTION 1

1.1 Background 1

1.2 The Program 2

1.2.1 Objectives 2

1.2.2 Approach 2

1.2.3 Organization 3

2. PHASE I ASSIMILATION OF PERTINENT INFORMATION 4

2.1 Survey 4

2.2 Results 4

2.2.1 Navy Concerns 4

2.2.2 Data Available or Work in Progress 5

2.2.3 Result of the Survey 6

3. PHASE II STRUCTURAL INTEGRITY ANALYSIS 8

3.1 Introduction 8

3.1.1 The J Integral 8

3.1.2 R Curve 9

3.2 Stability Analysis 10

3.2.1 Specimen in Series with a Spring Displacement Controlled Conditions 11

3.2.2 Alternate Physical Interpretation of the Instability Condition 13

3.2.3 Specimen in Parallel with Spring Load-Controlled Conditions 15

3.2.4 J-T Diagrams 19

3.3 Methodology for Structural Analysis 20

3.3.1 Calibration Curves 21

3.3.2 Material Resistance to Crack Growth 22

3.3.3 Methodology 23

3.4 Discussion 24

4. APPLICATIONS 27
4.1 Introduction 27
4.2 Model 28
4.3 Monotonic Loading 29
4.3.1 Tensile Material Properties 29
4.3.2 Elastic Plastic Formulation Calibration Curves 29
4.3.3 Material Response to Crack Growth 31
4.3.4 Computer Program 31
4.3.5 Results and Discussion 32
4.4 Cyclic Loading 36
5. FINAL DISCUSSION AND RECOMMENDED RESEARCH 38
6. ACKNOWLEDGEMENTS 40
7. REFERENCES 41
8. TABLES AND FIGURES 44

1. INTRODUCTION

1.1 Background

The assurance of safe and reliable structural performance of critical components, structures, and equipment subjected to adverse loading conditions has always been a matter of vital concern to both the U.S. Navy and the Westinghouse Electric Corporation. The capability to conduct appropriate structural integrity analyses takes on an added importance when new equipment, designs, materials, inspections and fabrication procedures are concerned.

In these situations there is little or no service experience to rely upon; hence, a thorough structural integrity analysis, incorporating all of the interacting factors must be included as a major element in the overall plan. Such analyses should take advantage of the most advanced technology areas that are applicable to the situation of concern; in this case modern fracture mechanics technology offers a unique and directly applicable capability.

Early developments of fracture mechanics focused on plane-strain or essentially linear elastic fracture conditions (LEFM) and on relatively high strength brittle materials such as aircraft structures, missile cases, gun tubes, etc. Soon the technology was extended to include fatigue and stress corrosion crack propagation. Later on, because of the recognized limitations in the applicability of LEFM, effort was devoted to extend the fracture mechanics technology to encompass situations involving considerably more plasticity than is permissible under LEFM conditions. As a result the break through came in the form of the path independent J-integral, a field parameter analogous to K in LEFM. The general usefulness of the technology has thus been extended to a much broader spectrum of applications and

materials: lower strength, higher localized stress regions, low cycle fatigue and creep controlled crack growth. Even more recently, the technology has taken another major step forward with the advent of J resistance curves, tearing modulus concepts and tearing instability models. These recent developments offer the capability to predict the permisable amounts of stable crack growth in the ductile temperature regime, and the eventual instability conditions for the catastrophic failure of the structure by ductile tearing under fully plastic conditions. More importantly these recent advances in technology offer the promise of enabling the design of structures and selection of materials so as to avoid any possibility of failure due to ductile tearing instability.

In short, fracture mechanics provides engineers with a powerful new tool for more effective design pertaining to structural reliability.

1.2 The Program

1.2.1 Objectives

In this spirit, the Westinghouse Electric Corporation conducted the present program with the major objective of assisting the Navy in developing and applying advanced fracture mechanics technology to ensure structural integrity in critical applications of titanium alloys. The specific objectives were

1) Development of methods for assessing Structural Reliability
2) Respond to Specific Navy Concerns
3) Recommendation of methods for implementing structural reliability procedures

1.2.2 Approach

In order to accomplish the mentioned objectives it was decided to use the following approach: the program was divided in two phases.

Phase I Assimilation of pertinent information

In this phase a comprehensive review of the currently available information and data needed for applying advanced fracture mechanics technology to structural reliability analysis as well as the concerns of the Navy was conducted. This review included such pertinent information areas as loading conditions and stresses involved, material properties, fabrication procedures and nondestructive inspection capabilities.

Phase II Structural integrity analysis

Phase II included the development of methods to assess structural reliability. After considering different candidates the best possible choice was proposed using the latest concepts in fracture mechanics methodology. The method was applied to different models.

1.2.3 Organization of the Present Report

This report is organized as follows. Phase I and Phase II are discussed in detail in Sections 2 and 3 respectively. In Section 4, the results of applying the proposed methodology to specific models are shown. In Section 5 a general discussion of the program and recommendations for future work are made. In Section 6, the help of Navy personnel is acknowledged. Finally, References, and Tables and Figures can be found in Sections 7, and 8 respectively.

2. PHASE I ASSIMILATION OF PERTINENT INFORMATION

2.1 Survey

An extensive survey was conducted to gather information and data. This survey included visits by the Westinghouse Program Team to different Navy facilities. The main points addressed in the survey were

a) Navy concerns. An adequate characterization was made of the different areas that concern Navy personnel.

b) Available information and data. A list of areas where experimental data exist or is being generated today was made.

2.2 Results

2.2.1 Navy Concerns

The first phase of this program is "Assimilation of pertinent information and data." To do this several meetings were held between members of the Westinghouse program team and Navy technical personnel at a number of different Navy facilities. Also Westinghouse participated in a ONR Ti-100 Workshop. As a result of these meetings, many areas were identified as having significance to the problem of structural integrity analysis for Ti-100 and questions were raised regarding these areas; a list of those follows.

1) Toughness - How much toughness is enough? How should toughness be characterized for structural analysis?

2) Dynamic Loading - What is the fracture behavior under dynamic loading rates? Can the parameters used for conventional fracture analysis also be used under dynamic loading?

3) Fatigue - Can fatigue to failure be analyzed? What is the effect of zero to compression loading on fatigue crack growth analysis?

4) Low Cycle Fatigue - What is the effect of this on crack initiation and growth?

5) Failure Criteria - No failure criterion is presently used. Can one be identified particularly for analyzing fatigue to failure?

6) Crack Growth Under Sustained Load - This phenomenon has been observed in the form of subcritical cracking and delayed failure. Is this related to environmental influences, creep or time dependent fracture toughness behavior?

7) Effect of Prestrain on Fracture Behavior - How is fracture toughness and other fracture behavior influenced by an initial prestrain?

8) Effect of Residual Stresses in Welds - How can these be measured and how can they be incorporated into a structural integrity analysis?

9) Thickness Effects - How are these accounted for in structural analysis?

10) Scale Models vs. Real Structures - How well do scale models predict fracture behavior in real structures? What models are the most appropriate ones to analyze?

11) Shop Fabrication vs. Field Fabrication - Are properties in field welded structures as good as those in shop welded structures?

12) Explosion Bulge and Tear Tests - What significance do these have; Can they be analyzed using advanced fracture approaches?

2.2.2 Data available or work in progress

In these meetings the present availability of experimental data and the work in progress in different areas were discussed. A list of those follows:

1) Dynamic vs Static J-R Curves

The effect of loading rate in the J-R curve.

2) J-R Curve and Toughness

Material toughness data and the possible effect of variables on those values, i.e., thickness, prestrain,etc.

3) Fatigue

Data fatigue crack growth for different conditions.

4) Stress corrosion cracking

Different aspects regarding the stress corrosion cracking

5) Sustained Load Crack Growth

Crack growth under a fixed load level in different conditions.

6) Creep

Studies and experimental work in creep and creep crack growth

7) Environmental Effects

The effect of environment on all of the above mentioned areas.

2.2.3 Result of the Survey

The specific results of the survey are listed above, however some general conclusions can be drawn

1) Qualitative vs Quantitative

The concerns and questions raised on the several issues are not quantitative rather they are of a qualitative nature. The question asked is whether some parameter would at all affect the result, rather than precisely how much. This shows that many concerns are of a basic nature.

2) Diversity of Concerns

The survey revealed that at different Navy locations and among people of different technical functions there was frequently a difference in interests, concerns and priorities.

3) Points Address Experimental Work

Most of the points of concern can only be answered by additional experimental work.

4) Points of Concern and Basic Research

Several points that were raised are subjects presently being addressed in basic fracture research. In fact, it is not just a question of how to apply known concepts to titanium, or how titanium behaves under certain conditions compared to other materials extensively tested. Instead, several points of concern are still an open question in other areas where fracture mechanics is much more advanced and has been extensively tested.

3. PHASE II STRUCTURAL INTEGRITY ANALYSIS

3.1 Introduction

3.1.1 The J Integral

Recognizing that the applicability of LEFM was necessarily limited, researchers in fracture mechanics endeavored to extend the technology to encompass situations involving considerably more plasticity than is characteristic of LEFM. The breakthrough came in the form of the path independent J-integral,[1] a field parameter analogous to K in LEFM. As a direct extension of linear-elastic behavior, J can be regarded as the strength of the stress-strain fields near the crack tip for nonlinear elastic materials.[2,3,4,5] Figure 1 illustrates the crack tip stress-strain field with J as the single parameter characterizing the strength of that field.

The ductile fracture can be divided into separate steps, Figure 2a. Each step can be represented on a plot of J versus ductile crack extension, Δa, which is labeled the R curve, Figure 2b. The point on the R curve where a blunted crack tip begins to tear in a stable manner has been labeled J_{Ic}. J_{Ic} marks the initiation of the ductile cracking behavior in a material and has been labeled as a material property. J_{Ic} is limited in use for structural fracture evaluation in that it often provides a too conservative evaluation of toughness. The stable crack advance shown in the R curve of Figure 2b, often provides useful structural life well beyond the J_{Ic} point. The R curve then becomes the representation of fracture toughness most useful for evaluating structural behavior.

3.1.2 R Curve

The concept of a crack growth resistance curve -- the R curve -- provides a useful general framework for understanding the relationship between specimen geometry effects and material behavior. This concept may be explained in the following manner: Consider a cracked body being monotonically loaded. Any fracture mechanics parameter -- such as G, J, K, crack opening displacement (COD), or crack opening angle (COA) — can be chosen to characterize the generalized crack driving force. The crack may start to grow in a slow-stable manner above a certain applied crack drive level. The R-curve represents a locus of equilibrium conditions where the crack will remain stable if the loading is stopped, and where the applied crack driving force is equal to the crack growth resistance of the material; i.e., G_I or J = R(MN-m/m^2) or K_I = KR(MPa/$m^{1/2}$). Unstable crack growth develops when the crack driving force increases at a greater rate than the crack growth resistance.

The R-curve concept has been successfully developed for use in the linear-elastic range, and the characterizing crack drive can be either K_I or G_I. Experiments have shown that in the dominant elastic/small-scale-plastic range, a crack growth resistance curve can be considered a material property. In stating this, the R-curve is proven to be independent of specimen geometry effects such as initial crack size, specimen width, or specimen type. Observed effects are dependent on the material thickness and test temperature, since these variables affect the basic material toughness behavior.

The first step in considering elastic-plastic and fully plastic R-curves is the choice of a suitable parameter to characterize the generalized crack driving force. J-integral and COD concepts were designed specifically for use up to the crack growth initiation point. After significant slow stable crack growth has developed, the use of these elastic-plastic methods must be justified. Hutchinson and Paris[6] showed that J can be used to characterize the crack growth process if the remaining ligament, b, in a J test specimen is large

enough so that a region of proportional strain field easily encompasses the local crack tip nonproportional strain field. They defined a material based length parameter, D, which they expressed as a function of the R-curve slope and J itself; that is, $D = J/(dJ/da)$. And then the size requirement is $b \gg D$ or $\omega = b/D \gg 1$. The required size of the proportional region before J is affected has not yet been well fixed.

The R curve based on J as the characterizing parameter is justified through the analysis of Hutchinson and Paris. It can therefore be used to assess the fracture stability of structural components; this analysis of structural stability is discussed in the following section.

3.2 Stability Analysis

Although the J-R curve concept is growing in acceptance and its use becoming more common, the question of whether a crack will grow stable or unstable remained unresolved until very recently. It was recognized that instability results from a lack of balance between the rate of increase of the applied drive force and that one of the material resistance to crack growth.

Recently, the basic implications of this concept were further explored by Paris et al.[7-8] and, as a result, it was demonstrated that the overall characteristics of the structure play a major role in instability and its effects have to be included in the rate balance mentioned. In this work, they introduced a non-dimensional quantity called the tearing modulus, T, that in general has the form:

$$T = \frac{E}{\sigma_o^2} \frac{dJ}{da} \tag{1}$$

where E is the elastic modulus and σ_o is the flow stress. If Equation (1) is evaluated using the J-Resistance curve of the material, the resulting T is the material tearing modulus T_{mat}. If instead, dJ/da in Equation (1) is calculated as the rate of change of crack drive or the

applied J, per unit virtual crack extension, with the condition of total displacement, δ_{tot}, kept constant (or other similar conditions specified), the resulting T is the applied tearing modulus T_{app}. And so following References[7-8], instability will occur when:

$$T_{app} \geq T_{mat} \tag{2}$$

Using the condition of total displacement constant, the compliance of the structure, C_M, is introduced into the analysis the T_{app} becomes a function of C_M. Consequently, according to the theory, Equation (2), instability is predicted provided the values of T_{mat} and expressions for T_{app} are known. In their original work, Paris et al. developed formulae for T_{app} for different configurations assuming perfect plasticity and that the crack grew under limit load conditions. They also performed the first experimental evaluation of the theory. In tests of three point bend specimens loaded in series with a spring bar of adjustable length, the compliance of the system, C_M, was varied from test to test, producing stable or unstable behavior in complete agreement with the theory.

The results were originally shown in a T_{mat} vs T_{app} plot, Figure 3. Each test is represented by its T_{mat} and T_{app} values. Open points correspond to unstable crack growth while filled points correspond to stable crack growth. Ideally, according to the theory, all open points (unstable) should lie to the right of the 45° line (region where $T_{app} > T_{mat}$), while the filled points (stable) should lie at the left of the 45° line (region where $T_{mat} > T_{app}$). The excellent agreement shown in Figure 3 was the first experimental verification of the tearing instability theory.

3.2.1 Specimen in Series with a Spring Displacement Controlled Conditions

Since this first work, significant effort was devoted to extend the same concepts in different directions. To better illustrate these concepts consider the example shown in Figure 4. A specimen is loaded

in series with a linear spring of constant $K_M = C_M^{-1}$, simulating the structure, in a displacement controlled test.

Hutchinson and Paris developed a general expression for T_{app} for this configuration

$$T_{app} = \frac{E}{\sigma_o^2} \left[\left.\frac{\partial J}{\partial a}\right|_{\delta} - \left.\frac{\partial J}{\partial \delta}\right|_{a} \left.\frac{\partial \delta}{\partial a}\right|_{P} \frac{1}{\left[C_M + \left.\frac{\partial \delta}{\partial P}\right|_{a}\right]} \right] \tag{3}$$

where δ is the displacement due to the crack and C_M is the compliance of the spring. All the terms appearing in the above equation are calibration functions, i.e., they don't bear any information regarding the material response to crack growth. These functions can be obtained from finite element analysis or experimentally from blunt notch specimen tests, and no "real" crack growth test is needed for their determination. This scheme has been used[7-8] to obtain T_{app} for different configurations of practical interest and, as was mentioned, instability can be predicted by comparing the value of T_{app} obtained from Equation (2) with the experimentally obtained T_{mat}.

Recently Ernst et al.[9,10,11] developed general formulae to evaluate both T_{mat} and T_{app} directly from a load-displacement (P-δ) test record giving, for the above case, respectively

$$T_{mat} = \frac{E}{\sigma_o^2} \left[\left.\frac{\partial J}{\partial a}\right|_{\delta} - \left.\frac{\partial J}{\partial \delta}\right|_{a} \left.\frac{\partial P}{\partial a}\right|_{\delta} \frac{1}{\left(\left.\frac{\partial P}{\partial \delta}\right|_{a} - \frac{dP}{da}\right)} \right] \tag{4}$$

$$T_{app} = \frac{E}{\sigma_o^2} \left[\left.\frac{\partial J}{\partial a}\right|_{\delta} - \left.\frac{\partial J}{\partial \delta}\right|_{a} \frac{1}{\left.\frac{\partial P}{\partial \delta}\right|_{a} + K_M} \right] \tag{5}$$

This formulation allows a direct comparison between the T_{mat} vs T_{app} values. The instability condition can now be found directly defining

$$\Delta T = T_{mat} - T_{app} \tag{6}$$

Instability will result when

$$\Delta T < 0 \tag{7}$$

or using Equations (4) and (5).

$$\Delta T = -\frac{E}{\sigma_o^2}\left[\left.\frac{\partial P}{\partial a}\right|_\delta \left.\frac{\partial J}{\partial \delta}\right|_a \left(\frac{1}{\left.\frac{\partial P}{\partial \delta}\right|_a - \left.\frac{dP}{d\delta}\right|} - \frac{1}{\left.\frac{\partial P}{\partial \delta}\right|_a + K_M}\right)\right] < 0 \tag{8}$$

noting that $\left.\frac{\partial P}{\partial a}\right|_\delta < 0$

$$\Delta T < 0 \text{ if and only if} \tag{9}$$

$$-dP/d\delta > K_M \text{ for the instability condition}$$

Thus according to the theory, instability will ensure when $\Delta T < 0$ and that will happen if and only if $-dP/d\delta > K_M$.

3.2.2 Alternate Physical Interpretation of the Instability Condition

The condition for instability can be obtained using a different approach.

Consider the P-δ record of a bend specimen tested under displacement control, and the correponding calibration (nongrowing crack) curves as shown in Figure 5a.

It is assumed that the fracture process is described in terms of the J-R curve; that is, every point in the P-δ record has associated a value of J, J_i and a value of a, a_i which are connected according to the J-R curve.

Suppose now that an identical specimen (same a/W) is tested, this time in series with a spring (as described before), Figure 5b. It can be seen that the effect of the spring on the calibration functions is just to shift every point in Figure 5a to the right by an amount

$$\delta_M = PC_M$$

or

$$\delta_{A'} = \delta_A + P_A C_M \tag{10}$$

$$\delta_{B'} = \delta_B + P_B C_M \tag{11}$$

where P_A and P_B are the loads at Points [A-A'] and [B-B'], respectively. Note that corresponding points, [A-A'], [B-B'], etc., have the same value of J(J depending on a/W and displacement only due to the crack, δ). Thus the resulting test record is expected to go through these corresponding points [A'],[B'], etc. in order to follow the J-R curve as before. Combining Equations (10) and (11) gives

$$\delta_{B'} - \delta_{A'} = \delta_B - \delta_A + C_M(P_B - P_A) \tag{12}$$

is important to note that for the portion of the test record where $P_B - P_A < 0$ (dropping part), the relative distance of subsequent points is diminished by the addition of the spring

$$\delta_B - \delta_A > \delta_{B'} - \delta_{A'} \text{ if } P_B < P_A \tag{13}$$

In fact, if enough compliance is added, this relative distance can even turn out to be negative; that is, Point [B'] lying to the left of [A']. If this is the case the test record would have to go backwards (in δ) to pass through [B'] in order to follow the J-R curve. But this is not compatible with the boundary condition, which asks for a monotonically increasing displacement. Thus, the test record gets as near to Point [B'] as it is allowed to (vertical drop), corresponding to unstable growth.

The conditions for stability can be then expressed as

$$\delta_{B'} - \delta_{A'} < 0 \text{ unstable}$$

$$\delta_{B'} - \delta_{A'} > 0 \text{ stable} \tag{14}$$

Replacing Equations (10) and (11) in the preceding expression gives

$$\delta_{B'} - \delta_{A'} = \delta_B - \delta_A + (P_B - P_A)\, C_M < 0$$

$$\frac{\Delta\delta}{\Delta P} < - C_M \tag{15}$$

$$C_M^{-1} = K_M < - dP/d\delta \text{ for instability}$$

This condition was found on a completely general basis with no need to mention J or even crack length. It is exactly the same as that one of Equation (9) found from tearing instability theory. As a result the condition $\Delta T < 0$ is a necessary and sufficient one for instability. Thus, the tearing instability theory has been proven to be always valid.

3.2.3 Specimen in Parallel with Spring Load-Controlled Conditions

It is well recognized that the structural member is normally constrained by the structure in such a way, that neither an exclusively load-controlled, nor a displacement-controlled situation is realistic, but more likely a mixed one where the stiffness of the rest of the structure K_M has to be taken into account. In the last section it was shown that by adding a spring in series with the specimen in a displacement controlled test, the structure can be simulated and in fact, the whole range from load control to displacement control can be covered by just changing the stiffness of the spring K_M. Nevertheless, that is not the only possible way of ranging from one end to the other. In fact, there are situations where the structure is in an intermediate loading condition which cannot be represented by the above mentioned model. Namely redundant structures where several members are sharing the overall applied load: stiffened plates or pipes, set of structural supporters, cables, etc. The stability of crack growth problem for this type of structures was the subject of a recent paper by Paris et al[12], where they developed the so-called Fracture Proof Design Concept. According to this concept structural parts can be designed in such a way as to guarantee stable crack growth even under

load-controlled conditions. To better illustrate these concepts consider a specimen in parallel with a spring of constant K_M simulating the structure, subjected to load controlled conditions, as shown in Figure 6. For this case Ernst[11] obtained the expression for T_{mat} and T_{app}.

$$T_{mat} = \frac{E}{\sigma_o^2} \left[\left.\frac{\partial J}{\partial a}\right|_{\delta} - \left.\frac{\partial J}{\partial \delta}\right|_{a} \frac{\left.\frac{\partial P}{\partial a}\right|_{\delta}}{\left(\left.\frac{\partial P}{\partial \delta}\right|_{a} - \frac{dP}{d\delta}\right)} \right] \tag{16}$$

$$T_{app} = \frac{E}{\sigma_o^2} \left[\left.\frac{\partial J}{\partial a}\right|_{\delta} - \left.\frac{\partial J}{\partial \delta}\right|_{a} \frac{\left.\frac{\partial P}{\partial \delta}\right|_{a}}{\left.\frac{\partial P}{\partial \delta}\right|_{a} + K_M} \right] \tag{17}$$

This equation is the general expression for T_{app} for a specimen in parallel with a spring (structure) under load controlled conditions. The instability condition can be obtained by comparing Equations (16) and (17) giving

$$\Delta T = T_{Mat} - T_{app} < 0 \tag{18}$$

if and only

$$-dP/d\delta > K_M$$

for instability

Following a similar line to the last section, the instability condition can be obtained from the P-δ record itself.

Consider the P-δ record of a specimen tested under displacement control as shown in Figure 7a. Suppose now that an identical specimen is tested in parallel with a spring of compliance C_M (or stiffness $K_M = C_M^{-1}$). The displacement underwent by the specimen, and that one of the spring δ_M are the same

$$\delta = \delta_M \tag{19}$$

On the other hand, according to the principle of equilibrium, the load held by the specimen, P, plus the load held by the spring P_M, give the total externally applied displacement P_{tot}

$$P_{tot} = P + P_M \tag{20a}$$

As a consequence, the second specimen test record (P_{tot}, δ) shown in Fig. 7b, will be just the result of shifting every point of the original P-δ record up in load by an amount

$$P_M = K_M \, \delta \tag{20b}$$

As before, if two generic points A and B in Fig. 7a are considered, with coordinates (δ_A, P_A) and (δ_B, P_B) respectively, the addition of the spring will shift them to (δ_A, $P_{A'}$) and (δ_B, $P_{B'}$), with

$$\begin{aligned} P_{A'} &= P_A + K_M \, \delta_A \\ P_{B'} &= P_B + K_M \, \delta_B \end{aligned} \tag{21}$$

Combining the above equations one gets Equation (22) here

$$(P_{B'} - P_{A'}) = (P_B - P_A) + K_M \, (\delta_B - \delta_A) \tag{22}$$

The above expression can be regarded as the fundamental instability equation for load controlled systems. If points A and B were in the raising portion of the P-δ record ($P_A > P_B$) the addition of the spring causes an increase in the load difference due to the fact that the second term in the right hand side of Equation (22) is positive.

$$(P_{B'} - P_{A'}) > (P_A - P_B) \tag{23}$$

If the points A and B were in the dropping portion of the P-δ record ($P_A > P_B$), the addition will also cause an increase in the load difference for the same reason as before.

$$(P_{B'} - P_{A'}) > (P_B - P_A) \tag{24}$$

In fact, if the second term in the right hand side of Equation (22) is big enough the relative difference in load can turn to be positive $P_{B'} - P_{A'} > 0$, and that means <u>an always increasing curve in load</u>. The required value of K_M to produce this behavior can be obtained from Equation (22)

$$\begin{aligned} (P_{B'} - P_{A'}) &= (P_B - P_A) + K_M (\delta_B - \delta_A) > 0 \\ -\frac{P_B - P_A}{\delta_B - \delta_A} &< K_M \\ -dP/d\delta &< K_M \end{aligned} \tag{25}$$

to produce a monotonically increasing curve.

Note that if the resulting $P_{tot} - \delta$ record is a monotonically increasing curve, it is irrelevant whether the test is run under load or displacement controlled conditions i.e., the test will be stable regardless of these conditions. Thus, Equation (25) represents the fundamental condition for stable behavior under load controlled conditions, and the minimum value of K_M that satisfies it, is the minimum value of stiffness required to produce a monotonically increasing curve and thus prevent instability. As a result the instability conditions are

$$\begin{aligned} -\, dP/d\delta &< K_M \quad \text{stable} \\ -\, dP/d\delta &> K_M \quad \text{unstable} \end{aligned} \tag{26}$$

Note that this condition is exactly the same as that one of Equation (18) derived for a completely different situation; in both cases stable behavior will be guaranteed if and only if

$$-dP/d\delta < K_M \tag{27}$$

As in the last section, note that this condition is completely general and agrees with that one obtained from the tearing instability theory. This condition obtained from the tearing instability theory agrees with Equation (18) obtained on a completely general basis, based on nothing else but the principle of equilibrium. As a result, the tearing instability theory has proven to be always valid for load controlled conditions in the sense that instability will occur if and only if $\Delta T < 0$. Note that as before, if any other parameter $X = X(\delta, a)$ was used instead of J, the resulting X-based tearing moduli, T_{matX} and T_{appX}, will provide an automatically validated tearing instability condition.

Finally, it is to be noted that Equations (15) and (27) <u>are the same</u> although they represent completely different situations. The former was obtained for a specimen in series with the spring under displacement control, while the latter was obtained for a specimen in parallel with the spring under load controlled conditions.

3.2.4 J-T Diagrams

In the last sections attention was devoted to the development of formula for T_{app} for different situations. Although since the original work of Paris et al.[7-8], significant effort was also devoted to experimentally verify the tearing instability theory. Joyce et al.[13], Vassilaros et al.[14] and Kamimen et al.[15] among others conducted several experimental programs to do this. The basic philosophy has been the same as that one of the initial work of Paris et al.[7-8]; select a certain material-specimen geometry combination and run a series of displacement controlled tests of specimens in series with a spring whose compliance could be changed from test to test. Values of T_{mat} were

obtained as the normalized slope of the J-R curves and T_{app} values were obtained using some of the different schemes[6-11,16].

As was mentioned earlier at the beginning, the results were reported in a T_{mat} vs T_{app} plot similar to that of Figure 3, but later on, it was realized that in general neither T_{mat} nor T_{app} were constant in a given test. As a consequence, the results were shown in a J-T plot as shown in Figure 8. Slopes of the J-R curves were obtained at different J levels and after normalized replotted in a J vs T_{mat} frame. At the same time, using some of the schemes mentioned above values of T_{app} were obtained for different J levels and also plotted in the J-T frame. Every time that the two curves intercepted, instability was expected to occur at the intersection of the two curves; if the test were stable, the two curves should not intersect. If that was the case, instability was properly predicted by the tearing instability theory and thus the latter was said to be validated. The results, as predicted by the last section analyses, have proven to always validate the tearing instability theory.

3.3 Methodology for Structural Analysis

In the previous section the solution to the ductile fracture stability problem in a structure was given with the model of a test specimen in series or parallel with a spring. The test specimen represents a cracked component in a structure. It provides the resistance to increased crack extension. The spring in series represents the driving force tending to pull the structure to instability in a displacement limited structure. The spring in parallel represented redundant components resisting instability in a structure under applied loading. The problem of predicting instability in the structure is simple if the cracked component is identical in geometry to the laboratory specimen used to generate fracture resistant R curves. The problem to be solved in providing a methodology for structural analysis is that of predicting stability when the cracked component represents a different geometry from that of the test specimen. This problem can be

solved without conducting a test for each new geometry if two sets of information can be generated for that new cracked geometry. They are the calibration functions for the geometry which relate load, displacement and J as a function of crack growth. The second piece of information is the materials resistance to crack extension which is given by the R curve for the cracked structural geometry.

3.3.1 Calibration Curves

The calibration functions can be obtained from the load versus displacement behavior for the non-growing crack. One method for obtaining the calibration curves for a given cracked geometry is by the Shih-Hutchinson estimation procedures.[17-18] This procedure allows displacement and J to be calculated as a function of load and crack length. Inputs needed for this estimation procedure are the tensile properties of the material including the elastic modulus, E, the strain hardening exponent, n, and the proportionality constant, α, in the Ramberg-Osgood representation of hardening behavior. All of the constants can be obtained from a tensile test which measures the true stress-strain behavior.

The Shih-Hutchinson estimation procedure has been applied to a number of different cracked geometries using the finite element calculation method. The results of these calculations are summarized in a Handbook published by the Electric Power Research Institute.[19] Although this Handbook does not cover all possible geometries of interest and the accuracy of the estimation procedure itself has not been assessed experimentally, it does represent a viable method for obtaining calibration curves for many different types of cracked geometries.

The first part needed to apply the methodology, that of determining calibration curves for the cracked structure, has been solved by the estimation procedure. The results are available in handbook form and can be used by a competent engineer.

3.3.2 Material Resistance to Crack Growth

The second piece of information needed to apply the methodology is the R curve for the material and cracked geometry used in modelling the structure. This is a more difficult piece of information to obtain. It is known that R curves may be geometry dependent so that one determined from a laboratory test specimen may not be appropriate the cracked geometry which represents the structure. What is needed is a way to represent the R curve as truly a material property independent of all specimen geometry considerations. One step toward establishing the R curve as a material property was taken in specifying limitations for J controlled crack growth.[6] This approach stated that a geometry independent R curve can be developed on a laboratory test specimen which is appropriate for the cracked structural geometry if certain limitations can be met for both the laboratory specimen geometry and the cracked structural geometry.

Unfortunately, the limitations are not often met for typical materials used in building structures. A significant step in developing a geometry independent R curve came from the work of Ernst[20] in which he suggested a modified J parameter, J_M, which could be used to characterize the R curve behavior. R curves plotted with J_M were not subject to the same limitations imposed on the traditional deformation J-R curve representation.

Experimental data obtained in a program for the Electric Power Research Institute were used to show the adequacy of this approach. The program is described in detail in References[21-22]. Basically, it consisted of the R-curve testing of compact tension specimens (CT) of different planar sizes, thickness B and crack aspect ratio a/W, of a A508 Class 2 steel at 400°F.

Out of the large test matrix some specimens were selected for this study. These specimens were geometrically similar. All of them had an a/W = 0.6 and the thickness B was half of the total width W in all cases. The overall size ranged from 1/2T (W = 1 in) to 10T (W = 20 in).

The resulting J-R curves showed consistency at the early stages but, as expected, the different curves start deviating when the crack length increment Δa was significant compared to the ligament b.

The J-Δa curves were then converted to J-T plots. The result is shown in Figure 9. Here the differences between specimens are more obvious than in the regular J-R curve plot. It can be seen for lower T_{mat} (higher J) the "peeling off" of the smaller specimen curves occur. In fact, as was mentioned before for some specimens, T_{mat} is close to zero (even negative for the 1/2T ones). The same data were replotted using the J_M in a J_M-T_{Mmat} frame. Using for J_M and T_M

$$J_M = J_D + \int_{a_o}^{a} (1 + 0.76\ b/W)\ \frac{J_{pl}}{b}\ da \tag{28}$$

$$T_{Mmat} = \frac{E}{\sigma_o^2}\ \frac{dJ_M}{da} = T_{mat} + \frac{E}{\sigma_o^2}\left(\frac{1 + 0.76\ b/W}{b}\right) J_{pl} \tag{29}$$

As can be seen in Figure 10, all the curves collapse into one when J_M and T_{Mmat} are used, even for the last points of the smallest specimens. This basically means that J_M is correlating data for situations well beyond the so-called J controlled crack growth and crack extension up to 30% of the initial remaining ligament. This basically means that J_M is a better parameter to use for describing the material resistance to significant crack growth, and that its use for R curve representation makes maximum meaningful use of the information obtained from small specimens, well beyond the J controlled crack growth regime with no unnecessary reduction in the predicted toughness capability.

3.3.3 Methodology

When the two components needed in applying the methodology are determined (the calibration curves and the R curve for the cracked geometry representing the structure) the complete response of that structure to an applied loading can be determined. From this response

load versus displacement plots or J versus T diagrams can be obtained. The degree of stability of the structure and load capacity can be assessed.

The complete methodology is represented by a flow diagram in Figure 11. The structural cracked geometry model is taken with the material tensile properties to determine the calibration functions for that geometry. The R curve determined from a laboratory test specimen is represented in the J_M versus Δa format. This represents the geometry independent material property needed to assess the resistance to crack growth in the structural cracked geometry. The calibration curves and the R curve are then combined to produce load versus displacement or J-T curves for the model geometry. From these maximum load bearing capacity and stability of the structure are assessed. These can then be compared with the design requirements for the structure to determine whether the material toughness is adequate. Inadequate toughness would require that some point in the initial input be changed. This could be a modification of design requirements, the selection of a material with superior toughness or even a reanalysis of the structure using a more refined model for the cracked component in the structure.

3.4 Discussion

The methodology presented here represents in principle a complete approach to assessing the load bearing capacity and stability characteristics of any cracked structural geometry. In practice there are many steps in the methodology which need further assessment and development.

The determination of the calibration functions is the most advanced part of the method. The Handbook[19] containing the Shih-Hutchinson estimation procedure solutions provides the information needed to develop calibration curves. However, the number of solutions in the Handbook is presently limited and may not exist for a given structural model. Methods for adapting a solution to a different

geometry or combining solutions to best fit a structural model have not been developed. Also the solutions in the handbook were developed by finite element computations and their accuracy has not been verified independently by another method such as an experimental evaluation. Nevertheless, the Handbook solutions represent the best approach presently available for developing calibration curves for models of cracked structural components.

The R curve evaluation for the structural model represents the most difficult part of applying the methodology. The method developed by Ernst[20] representing the R curve with the modified J, J_M, is the most promising approach to developing a geometry independent material property. However, this approach is still in the early stages of development and cannot be applied with complete confidence. Certainly this approach would have inherent limitations and these have not been determined.

This methodology does present a complete approach for evaluating a cracked structure, although in practice there are some steps that need further work.

First of all it is to be noted that although the methodology was presented in general, its use was exemplified mainly for the case of slow monotonic loading, assuming that the material properties do not change with time. Obviously there are other mechanisms of deformation and fracture such as creep, fatigue, rate dependent monotonic loading, environmentally assisted crack growth, and all the possible combinations of the above mentioned. Nevertheless, the methodology presented here, still represents a complete approach for evaluating the cracked structure, if the correct information regarding material response to deformation and crack growth for the particular mechanism is input in the central and right columns of Fig. 11 respectively. In other words, once the mechanism is determined, the two pieces of information needed are still the same: the calibration functions or material response to deformation and resistance curve or material response to crack growth, obviously,

obtained for the corresponding conditions. But in essence the methodology as presented does represent a complete approach for cracked structures evaluation.

4. APPLICATIONS

4.1 Introduction

In the last section the elastic plastic fracture mechanics methodology was presented. This scheme represents a complete approach for evaluating a cracked structure in terms of its capacity to bear load, displacement and energy and its tendency for instability.

It was mentioned in the last subsection that although it had been somewhat emphasized the aspect of slow monotonic loading, as an example, the approach can be used for any other mechanism, provided the necessary, pertinent information regarding material response to both deformation and crack growth is available. When more than one mechanism is present a study regarding how the different effects interact between themselves is needed, which means that further work both experimental and analytical has to be done.

One of the outputs of the presented methodology is that it clearly shows how unnecessarily conservative the design concept of J_{Ic} really is; and in turn allows the possibility of benefiting from the extra toughness of the material developed with crack growth. This is precisely the subject of this section. Basically it consists of a very detailed follow up of the methodology, not so much to show absolute numerical values but rather to exemplify with a sample model what the method can do in terms of making maximum use of the toughness that the material really has.

Finally, some effort was also directed to the fatigue crack growth response of the model.

4.2 Model

As was mentioned before, the first step in the methodology is to decide upon the model to use. This choice has to consider two aspects: on one hand one wants the model to represent as close as possible the real structure, but on the other hand there are usually problems regarding the existence of solutions (i.e. calibration functions in this case), the full understanding of the physics of the problem or the number of variables to handle. Thus any model is always to a certain degree an idealized representation of reality, that usually neglects part of it due to the existence of the mentioned limitations. In this case the structure is a cylinder with a wall thickness W = 4 in., and inside radius R = 200 in. with circumferential stiffners at a distance S = 40 in apart subjected to external pressure. The cracks, located at different locations, are considered part through the wall thickness and are subjected to multiple loads that are nonproportional and produce mixed mode loading (I and II).

The simplest case, and probably the most important one is that of a part through the wall crack located in the circumferential direction, midway between two stiffners. The crack aspect ratio, depth to length is (2c/a) = 10, Fig. 12. Even for this situation, there is no available finite element solution.

Thus, since the development of such solutions was not part of this program, it was decided to use the closest solution available in the EPH. The choice was a simple edge bar subjected to three point bending. The span was S = 40 in. and the width was W = 4 in.

Note that for a part through crack of an aspect ratio as big as 10, it can be considered as infinite ($2c/a \rightarrow \infty$) for practical purposes regarding the crack drive force at the vortex (deepest point). Also note that since $R/t \approx 50$, the curvature of the shell can be neglected for that crack.

The fact that the stiffners are attached to the structure (that is not a simple supported situation) can be simulated in principle by considering springs at the ends of the bar.

4.3 Monotonic Loading

4.3.1 Tensile Material Properties

It was assumed that the material follows a Ramberg- Osgood law given by

$$\frac{\varepsilon}{\varepsilon_o} = \frac{\sigma}{\sigma_o} + \alpha \left(\frac{\sigma}{\sigma_o}\right)^{1/n} \tag{30}$$

where σ_o and ε_o are the yield strength and yield strain respectively.

The values of these constants, provided by the Navy, are

$$\begin{aligned} E &= 17.5 \times 10^6 \text{ psi} \\ \sigma_o &= 110{,}000 \text{ psi} \\ \alpha &= 1 \\ n &= 10 \end{aligned} \tag{31}$$

4.3.2 Elastic Plastic Formulation. Calibration Curves

Once the geometry has been selected and the tensile material properties are available, the next step in the methodology of Fig. 11 is to obtain the calibration functions through an elastic-plastc formulation. Here the Elastic Plastic Handbook (EPH)[19], that follows the original scheme of Hutchinson and Shih [17,18], was used. In the EPH the solutions are presented as follows. First consider a material that obeys a constitutive law of the pure power type

$$\frac{\varepsilon}{\varepsilon_o} = \alpha \left(\frac{\sigma}{\sigma_o}\right)^{1/n} \tag{32}$$

For this material, the expressions for J and load point displacement δ (called Δ in the EPH), or fully plastic solutions are given as

$$\begin{aligned} J &= \alpha\, \sigma_o \varepsilon_o\, b\, h_1(a/W,n)(P/P_o)^{n+1} \\ \delta &= \alpha\, \sigma_o \varepsilon_o\, a\, h_3\, (a/W,n)(P/P_o)^{n} \end{aligned} \tag{33}$$

where P is the load per unit thickness, a is the crack length, b is the remaining ligament, and P_o is the limit load per unit thickness for a perfectly plastic material ($n = \infty$). The expression for P_o for plane strain is

$$P_o = 0.728\ \sigma_o\ b^2/L \tag{34}$$

whereas for plane stress P_o is

$$P_o = 0.536\ \sigma_o\ b^2/L \tag{35}$$

On the other hand if the material is linear elastic,

$$\frac{\varepsilon}{\varepsilon_o} = \frac{\sigma}{\sigma_o} \tag{36}$$

the elastic J, J_{el}, and the elastic δ, δ_{el} can be expressed as [23].

$$J_{el} = \frac{K^2}{E^1} = \frac{9P^2}{4WE'} \left(\frac{\pi a}{W}\right) \left(\frac{S}{W}\right)^2 F^2(a/W) \tag{37}$$

$$\text{with } F = \sqrt{\frac{2W}{\pi a} \tan \frac{\pi a}{2W}} \quad \frac{0.923 + 0.199\ (1 - \operatorname{Sin} \pi a/W)^4}{\cos \frac{\pi a}{2W}}$$

$$\delta = 6 \frac{P}{E'} \frac{a}{W} \frac{S}{W} \quad V_1$$

$$\text{with } V_1 = \left(\frac{a/W}{1-a/W}\right)^2 [5.58 - 19.57\ (a/W) + 36.82\ (a/b)^2 - 34.94\ (a/W)^3 + 12.77\ (a/W)^4] \tag{38}$$

Finally, when a material obeys a Ramberg-Osgood law Eq (30), the EPH estimates the total value of J and δ by adding the linear elastic expression plastically connected and the fully plasic solution. The latter consists of considering an effective crack length which is

$$a_{eff} = a + \phi\ ry$$

$$\text{with } r_y = \frac{1}{\beta\pi}\left(\frac{n-1}{n+1}\right)\left(\frac{K}{\sigma}\right)^2 \tag{39}$$

$$\phi = \frac{1}{1 + (P/Po)^2}$$

and $\beta = 2$ for plane stress and $\beta = 6$ for plane strain.

Giving thus

$$J = \frac{K^2}{E}(a_{eff}, P) + \alpha\ \sigma_o \varepsilon_o\ b\ h_1 (P/Po)^{n+1}$$

$$\delta = \delta_{el}(a_{eff}, P) + \alpha\ \sigma_o \varepsilon_o\ a\ h_3\ (P/Po)^n \tag{40}$$

In this study the plane strain solutions were used.

4.3.3 Material Response to Crack Growth

The material response to crack growth was characterized by the J-R curves provided by the Navy, for the three material conditions 0, 1 and 3% prestrain. These curves were obtained using 1T compact specimens (W = 2"), under static loading at room temperature. Moreover, the curves were replotted using the modified J, J_M, concept to give J_M vs Δa curves. The expression for J_M used (valid for CT specimens) was

$$J_M = J + \int_{a_o}^{a} \frac{(1 + 0.76\ b/w)\ J_{pl}}{b}\, da \tag{41}$$

where J_{pl} is the plastic part of J (total minus pure elastic). These plots are shown in Figures 13, 14 and 15.

4.3.4 Computer Program

The next step in the methodology of Fig. 11, is to combine the information regarding deformation (central column) and crack growth (right column) in the computer program that constructs the P-δ record or J-T diagrams for the untested geometry. The mechanics of the program developed for this purpose was as follows.

First, the calibration functions given by the EPH, the $J_M - \Delta a$ curve and the expression connecting J and J_M for the selected untested geometry were stored into the program. That is

$J = J(P,a)$	Calibration Curve
$\delta = \delta(P,a)$	
J_M - R curve	pairs (J_M, Δa)
$J_M = J + \int_{a_o}^{a} \frac{J_{pl}}{b} da$	Expression for J_M for 3 point bend specimen. (42)

After some value of the initial crack length was selected, the program increases the load P from 0 to the point where the corresponding J matches the first value of J_M in the R curve ($\Delta a = 0$). Then the program increments a_o by Δa and with this new crack length $a = a_o + \Delta a$, increases the load P from 0 to the point where the corresponding J is such that produces a J_M (through Eq (42) that matches the J_M-R curve for that Δa. The process goes on until the whole $J_M - \Delta a$ curve is covered.

Every time that the correct J is found the corresponding values of P and δ (or $J - T_{app} - T_{mat}$, or $J_M - T_{Mapp} - T_{Mmat}$) are saved and reploted to build the $P - \delta$ record of the untested geometry (or J-T diagram), which follows the $J_M - \Delta a$ curve.

4.3.5 Results and Discussion

The results of the application of the methodology to the example model are shown in Figures 16 through 23 and in Table I.

The first three figures, 16, 17 and 18 show the P-δ records for a_o = 0.5; 1.0; 1.5 and 2.0 inches using the J_M-Δa curve, for the three material conditions 0, 1 and 3% respectively.

The three subsequent figures, 19, 20 and 21 show the same plotting, using this time the deformation J-Δa curve.

In Figure 22, the P-Δ records for a_o = 1.5 in and the different material conditions are compared using the J_M - Δa resistance curve. Figure 23 shows plots of J vs T_{app} for the model with springs in parallel. The value of the spring constants per unit thickness were K_M = 10; 50 and 100 k lbs/in^2. The value of a_o was 1.5 in. A schematic of J vs T_{mat} is also shown.

In Table I, the results for all the cases run are summarized in terms of loads P and values of J. Three values of the load are compared: the one at J_{Ic}, and the maximum attained ones using the J - Δa and J_M - Δa curves. Note that the maximum attained load is not necessarily the maximum load that the structure can withstand.

Two values of J are compared: the J_{Ic}, and the last value of J_M used from the R curve i.e. the J_M corresponding to the last P obtained through the computer program.

From the figures it can readily be seen that in most cases, the available information in terms of material resistance to crack growth did not allow the program to attain the maximum load, P_{max}, that the structure can hold. As a consequence, the slope of the decreasing portion of the P-δ record dP/dδ, needed for stability calulations, could not be obtained either.

This basically means that the resistance curves provided were too short (in Δa) to obtain points in the P-δ record beyond P_{max}. In other words, the last point used from the J or J_M - Δa curves was not sufficient to get to P_{max}. Thus the values of J or J_M corresponding to P_{max} are even bigger than the last ones used, and those are already significantly bigger than J_{Ic}. This can be appreciated better by considering Table I. For every case run, the load at J_{Ic} is obtained with the maximum attained value by using the J_M - Δa curve. It can be concluded that the load that the structure can hold is at least up to 20% bigger than that predicted by the use of J_{Ic}. On the other hand, in

the last two columns of the table the value of J_{Ic} is compared with that of J_M for the maximum attained load. It can be concluded that the latter are bigger by a factor of 2 to 3. This fact clearly shows how important the extra toughness developed with crack growth is. The toughness available in the materials is really much bigger than J_{Ic}.

A word is in order here, regarding the R-curves of Fig. 13, 14, 15. These curves were obtained using 1T CT specimens, thus the amount of crack extension is roughly 10 to 15% of the initial uncracked ligament. This means that the investigators who obtained these curves, did the right thing in stopping the tests and those points, since it was believed at the moment that the amount of crack extension should not exceed 10% of the ligament in order to keep the crack growth under the so-called J controlled conditions.

This point emphasizes the advantages that J_M provides. In fact, as shown, J_M can be used even for amounts of growth of 30% of the initial ligament. This means that much longer (in Δa) curves can be obtained from the same specimen size. Thus allowing the evaluation of a much larger structural parts (like in this case).

On the other hand, by looking at Fig. 22, it can be concluded that the material condition did not make much difference in terms of the obtained P-δ records. Although it is emphasized here that the records shown are only a portion of the complete ones, and presumably the differences are more obvious in terms of load, displacement, and energy when longer R-curves are used and thus complete P-δ records are considered. At the same time, as can be seen by considering Eq (49), J is proportional to P^2 in the elastic regime and to P^{n+1} in the fully plastic one. Thus, for all cases, changes in J represent much smaller changes in P. Thus, moderate differences in resistance curves (due to material condition for example) are translated into much smaller ones in P-δ records.

Finally, following the spirit of Section 3.2 the model was considered loaded in parallel with springs of different constants to

simulate the rest of the structure. The intention of this part was to perform an instability analysis following Section 3.2, by measuring the unloading part of the P-δ record, $dP/d\delta$, and show that if a spring of enough stiffness issued in parallel with the model, the crack growth can be stable even under load controlled conditions, past maximum load.

Unfortunately, as was extensively discussed, the J-R curves provided where not long enough to even reach P_{max}, thus the slope of the decreasing part of the P-δ records could not be measured. In terms of J-T diagrams this means that the material line is not long enough to cross the applied line. In any event, as an example, J vs T_{app} values were calculated for a_o = 1.5 in using spring stiffness (per unit thickness) of 10, 50 and 100 k lbs/in^2, a schematic material line (the real on does not cross the J-T_{app}) is also shown.

In summary, it can be concluded that:

1) Available J-R curves are not long enough (in Δa) to characterize crack growth behavior in the model. (due to a restriction on Δa to have J-controlled crack growth conditions).

2) The newly developed J_M, allows one to greatly extend the range of valid data. As a result its use is recommended to make maximum use of the information obtained from laboratory specimens.

3) An elastic plastic methodology can be used to assess structural integrity in a model, determining its characteristics to hold load; displacement and energy input and its degree of instability. 4) The presented methodology makes full use of the real toughness of the material by considering also the extra one developed with crack growth. Specifically in this particular model used:

a) the load carrying capacity increases at least 5 to 30%,

b) the toughness increases by a factor of at least 2 to 3, by using the present methodology as opposed to the unnecessarily conservative J_{Ic} design criterion.

4.4 Cyclic Loading

In the last sections, the case of monotonic loading was treated extensively. This usually represents the case of accident conditions where loads are very high and small duration.

On the other hand, also important is the problem of service conditions where loads are not that high but are cyclically applied.

For the cyclic loading case, elastic plastic fracture mechanics methods can also be applied, and are really in order for situations where the loads are high enough to produce extensive yielding. If this is the case, as shown by Begley and Dowling[24], the parameter to use is ΔJ, which in turn is general enough to cover linear elastic situations also.

Thus, neglecting crack closure effects, for load excursions from zero to maximum ($R = 0$) ΔJ can be obtained by using Eq (40), simply replacing P by ΔP. Here, as an example, this methodology was applied to the model detailed above. Basically, a computer program was developed that calculated the number of cycles N required for a certain initial crack a_o to get to the critical a, a_c, for which $J = J_{Ic}$ (at P_{max}). Thus the corresponding material properties, J_{Ic} and the expression for da/dN in terms of J provided by the Navy were entered into the program

$$J_{Ic} = 580 \text{ lbs in/in}^2$$

$$da/dn = C\ (\Delta J)^r \tag{43}$$

with

$$C = 10^{-7}$$
$$r = 2$$

when a is measured in inches and J in lbs in/in^2.

As mentioned, the number of cycles to failure were calculated for different initial a_o. The results are shown in Fig. 24. As a final comment it can be said that the material response to fatigue, Eq. (43),

is the simplest possible one: there is no threshold level effects (so called region I) or the usual raise of the curve when it approaches J_{Ic} (so called Region III), nevertheless, if a more complicated law is in order, the computer program can be easily adapted to handle it.

5. FINAL DISCUSSION AND RECOMMENDED RESEARCH

In the previous sections the elastic plastic fracture mechanics to assess structural reliability of cracked structures was developed in general and applied to specific examples. The method incorporates new EPFM concepts through the use of a J based R curve and tearing instability analysis. The central feature of the methodology is a model of the cracked structural geometry which is combined with a spring in series or parallel for the stability analysis. The method is based on the analysis of the response of the structure to deformation, labeled the calibration curves, and the response of the material and structure to crack advance, the R curve.

The calibration curves are evaluated through the Shih-Hutchinson estimation procedure. Results for this procedure are available in an EPRI published Handbook. The R curve is evaluated as a geometry independent material property using the modified J_M approach developed by Ernst. By combining the R curve and the calibration curves a complete description of the fracture behavior can be given for the structural model. Such things as maximum load bearing capability and structural stability can be assessed.

The results obtained show that levels of toughness between 2 and 3 times more than the J_{Ic} point can be attained before reaching the instability point. In terms of load carrying capacity the benefit of this method represents at least an increase of 20%.

The methodology presented in the first section is not necessarily limited to slow monotonically increasing load at room temperature. In fact it can be used when other mechanisms of deformation and crack growth are operating, provided the correct material response to deformation (central column of Fig. 11) and to crack growth (right column of Fig. 11) are available.

In principle, situations of obvious interest for the Navy as creep, dynamic loading, Mode II loading, among others, can be treated using this methodology. However, there are some areas of uncertainty that further work, both analytical and experimental, is needed.

The Handbook[19] containing the Shih-Hutchinson estimation procedure solutions provides the information needed to develop calibration curves. However, the number of solutions in the Handbook is presently limited and may not exist for a given structural model. Methods for adapting a solution to a different geometry or combining solutions to best fit a structural model have not been developed. Also the solutions in the handbook were developed by finite element computations and their accuracy has not been verified independently by another method such as an experimental evaluation. Nevertheless, these Handbook solutions represent the best approach presently available for developing calibration curves for models of cracked structural components. The R curve evaluation for the structural model represents the most difficult part of applying the methodology. The method developed by Ernst[20] representing the R curve with the modified J, J_M, is a promising approach to developing a truly geometry independent material property. However, this approach is still in the early stages of development and cannot be applied with complete confidence. Certainly this approach would have inherent limitations and these have not yet been determined. Other geometries should be tested, and those limitations should be explored.

The effects of different variables affecting the J-R curve such as loading rate, sustained load, cyclic loading (very high cycles) among others and the combination of them should be studied.

In conclusion, the methodology developed does present a complete approach for evaluating a cracked structure. However, there are certain areas where further work both experimental and analytical is needed.

6. ACKNOWLEDGEMENTS

The authors acknowledge the support of the Office of Naval Research through Contract N00014-80-C-0655. Dr. O. Arora of DTNSRDC Annapolis was the contract monitor. The helpful participation of different individuals from the Navy is also acknowledged with thanks, among those John Gudas and Ivan Caplan from DTNSRDC Annapolis, and M. Krenzke, A. Wiggs and L. Gifford from DTNSRDC Carderock.

7. REFERENCES

1. J. R. Rice, "A Path Independent Integral and the Approximate Analysis of Strain Concentration by Notches and Cracks," Journal of Applied Mechanics, 35: 379-386 (1968).

2. J. W. Hutchinson, "Singular Behavior at the End of Tensile Crack in a Hardening Material," Journal of the Mechanics and Physics of Solids, 16 (1): 13-31 (1968).

3. J. R. Rice and C. F. Rosengren, "Plane Strain Deformation Near a Crack Tip in a Power Law Hardening Material," Journal of the Mechanics and Physics of Solids, 16 (1): 1-12 (1968).

4. J. A. Begley and J. D. Landes, "The J Integral as a Fracture Criterion," Fracture Toughness, ASTM STP 514, pp. 1-23 (1972).

5. J. D. Landes and J. A. Begley, "The Effect of Specimen Geometry on J_{Ic}," Fracture Toughness, ASTM STP 514, pp. 24-39, (1972).

6. J. W. Hutchinson and P. C. Paris, "Stability Analysis of J-Controlled Crack Growth," Elastic-Plastic Fracture, ASTM STP 668, pp. 37-64 (1979).

7. P. C. Paris, H. Tada, A. Zahoor, and H. A. Ernst, "The Theory of Instability of the Tearing Mode of Elastic-Plastic Crack Growth," Elastic-Plastic Fracture, ASTM STP 668, pp. 5-36 (1979).

8. P. C. Paris, H. Tada, H. A. Ernst and A. Zahoor, "An Initial Experimental Investigation of Tearing Instability Theory," Elastic-Plastic Fracture, ASTM STP 668, pp. 251-265 (1979).

9. H. A. Ernst and P. C. Paris, "Techniques of Analysis of Load Displacement Records by J-Integral Methods", Nuclear Regulatory Commission NUREG/CR-1222, January 1980; also available as H. A. Ernst, PhD Thesis, Department of Mechanical Engineering, Washington University (St. Louis, MO), December 1979.

10. H. A. Ernst, P. C. Paris, and J. D. Landes, "Estimation on J-Integral and Tearing Modulus T from a Single Specimen Test Record," Fracture Mechanics: Thirteenth Conference, ASTM STP 743, Richard Roberts Ed, American Society for Testing and Materials, 1981, pp. 476-502.

11. H. A. Ernst, "Some Salient Features of the Tearing Instability Theory," presented at the Second International Symposium on Elastic-Plastic Fracture Mechanics, ASTM, Philadelphia, October 1981.

12. Paris, P. C., Tada, H. and Baldini, S. E., "Fracture Proof Design" CSNI Specialists Meeting on Plastic Tearing Instability held at the Center for Fracture Mechanics, Washington University, St. Louis, MO., September 25-27, 1979. U.S. Nuclear Regulatory Commission Report, Nureg CP-0010, January 1980.

13. J. A. Joyce and M. G. Vassilaros, "An Experimental Evaluation of Tearing Instability Using the Compact Specimen," Fracture Mechanics: 13th Conference, ASTM STP 743, American Society for Testing and Materials, 1981.

14. M. G. Vassilaros, J. A. Joyce and J. P. Gudas, "Experimental Verification of the Tearing Instability Phenomena for Structural Materials," presented at the 14th National Symposium on Fracture Mechanics, Los Angeles, CA, July 1981.

15. Kanninen, M. F., Zahoor, A., Wilkowski, G. M., Abou-Sayed, I. S., Marschall, C. W., Broek, D., Sampath, S. G., Rhee, H. D., and Ahmad, J., "Instability Predictions for Circumferentially Cracked Type 304 Stainless Steel Pipes Under Dynamic Loading," Battelle's Columbus Laboratories Final Report to the Electric Power Research Institute on T118-2, in preparation, June, 1981.

16. Zahoor, A., "Tearing Instability of Elastic-Plastic Crack Growth", Ph.D. Dissertation, Washington University, St. Louis, MO, August 1978.

17. Hutchinson, J. W., Needleman, A. and Shih, C. F., "Fully Plastic Problems in Bending and Tension", published in the Proceedings of an ONR International Symposium on Fracture Mechanics, Washington, DC, September 1978.

18. Shih, C. F., "J Integral Estimates for Strain Hardening Materials in Antiplane Shear Using Fully Plastic Solution," Mechanics of Crack Growt., ASTM STP 590, American Society for Testing and Materials, 1976, pp. 3-26.

19. Kumar, V., German, M. D., Shih, C. F., "An Engineering Approach for Elastic-Plastic Fracture Analysis," Electric Power Research Institute, NP1931, July 1981.

20. Ernst, H. A., "Material Resistance and Instability Beyond J Controlled Crack Growth," presented at the Second International Symposium on Elastic Plastic Fracture Mechanics, October 1981, Philadelphia, PA.

21. McCabe, D. E., Landes, J. D., "J_R Curve Testing of Large Compact Specimens", presented at the Second International Symposium on Elastic Plastic Fracture Mechanics, Philadelphia, October 1981.

22. McCabe, D. E., Landes, J. D., Ernst, H. A., "An Evaluation of the J_R Curve Method for Fracture Toughness Characterization", presented at the Second International Symposium on Elastic Plastic Fracture Mechanics, Philadelphia, PA, October 1981.

23. Tada H, Paris P. C. and Irwin, G. R., "The Stress Analysis of Cracks Handbook", Del Research Corporation - 226 Woodsource, St. Louis, MO 63130.

24. Begley, J. A. and Dowling, N. E. "Fatigue Crack Growth During Gross Plasticity and the J-integral", Mechanics of Crack Growth, ASTM STP 590 American Society for Testing and Materials, pp. 82-103, 1976.

Dwg. 6446A72

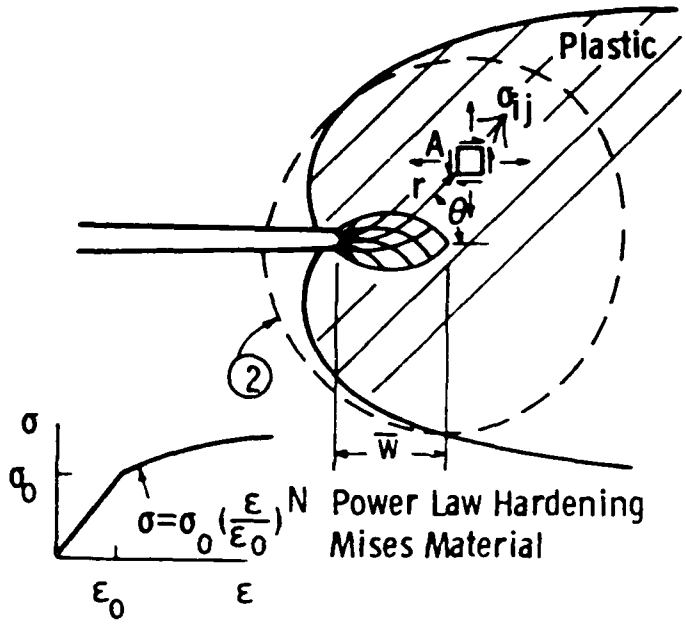

$$\sigma_{ij} = \sigma_0 \left(\frac{J}{r\,\sigma_0\,\varepsilon_0}\right)^{\frac{N}{1+N}} \bar{\Sigma}_{ij}(r, \theta, N)$$

$$\varepsilon_{ij} = \varepsilon_0 \left(\frac{J}{r\,\sigma_0\,\varepsilon_0}\right)^{\frac{1}{1+N}} \bar{E}_{ij}(r, \theta, N)$$

if $\bar{w} < r << $ planar dimensions

then: J is the intensity of the plastic field surrounding the crack tip

further: For the elastic case, $N = 1$, the above field equations give the same results as view 1.

where $J = G = \frac{K^2}{E}$

Fig. 1—Plastic crack tip field characterization, EPFM use J (or equivalent)

Dwg. 6446A72

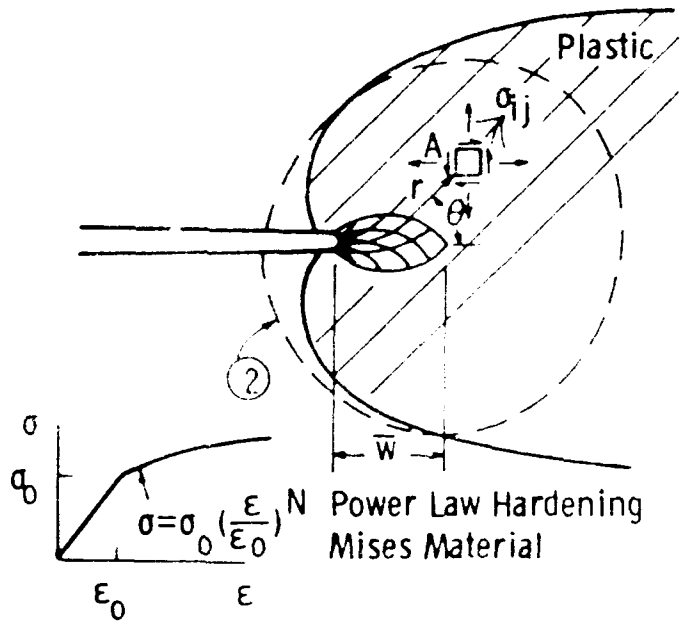

$$\sigma_{ij} = \sigma_0 \left(\frac{J}{r\,\sigma_0\,\varepsilon_0}\right)^{\frac{N}{1+N}} \bar{\Sigma}_{ij}(r, \theta, N)$$

$$\varepsilon_{ij} = \varepsilon_0 \left(\frac{J}{r\,\sigma_0\,\varepsilon_0}\right)^{\frac{1}{1+N}} \bar{E}_{ij}(r, \theta, N)$$

if $\bar{w} < r << $ planar dimensions

then: J is the intensity of the plastic field surrounding the crack tip

further: For the elastic case, N = 1, the above field equations give the same results as view 1, where $J = G = \frac{K^2}{E}$

Fig. 1—Plastic crack tip field characterization, EPFM use J (or equivalent)

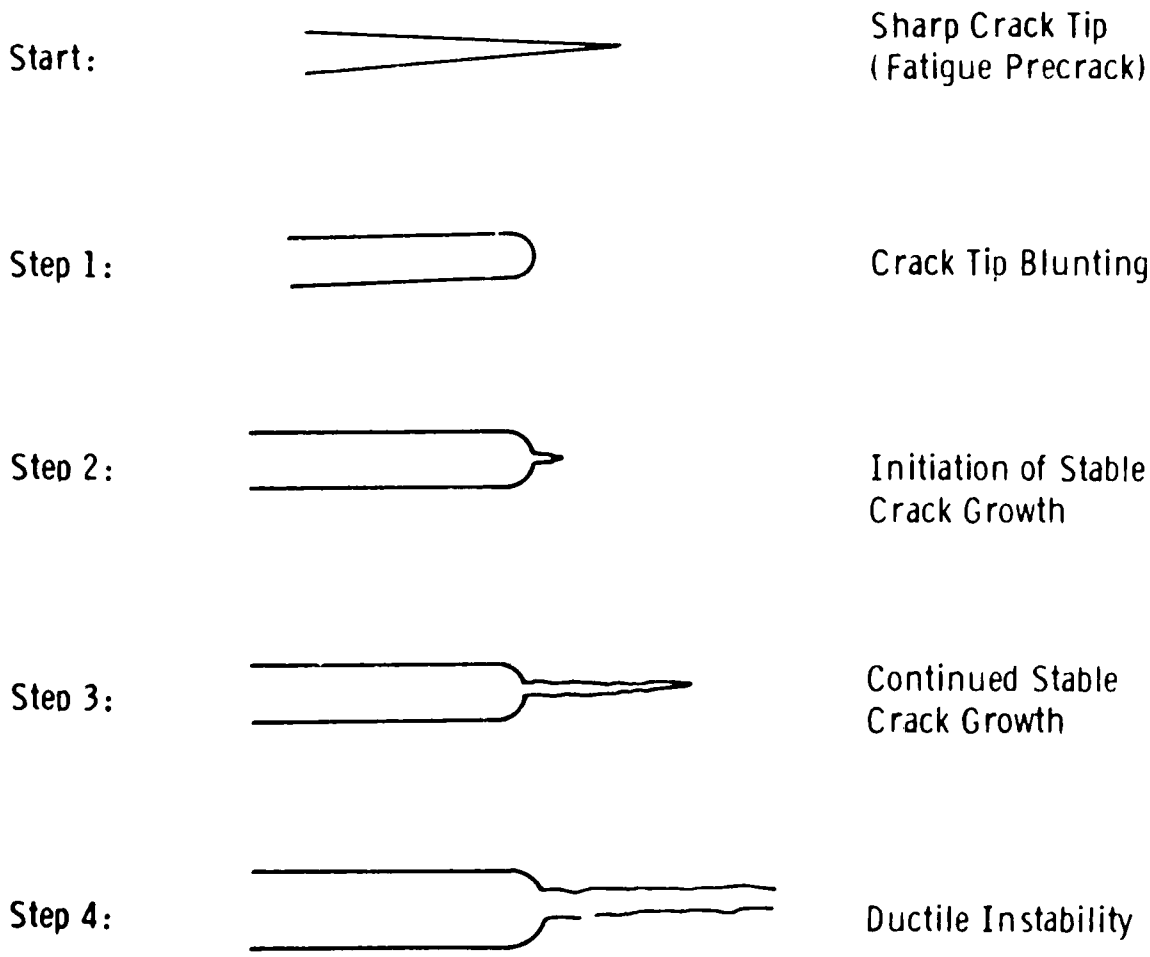

Fig. 2a—Four steps in ductile fracture process

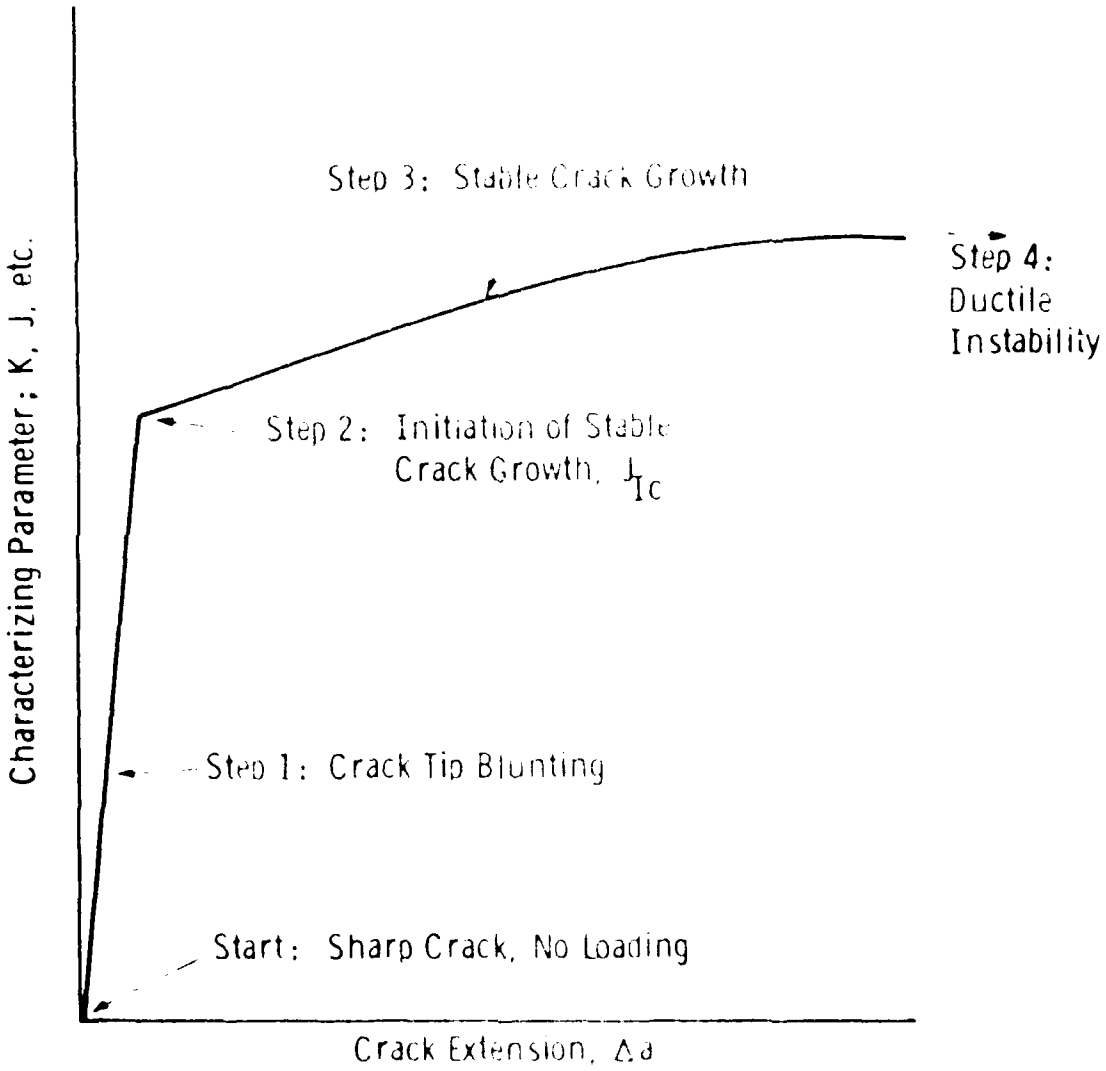

Fig. 2b—Four steps of ductile fracture process on an R-curve

Curve 597393-A

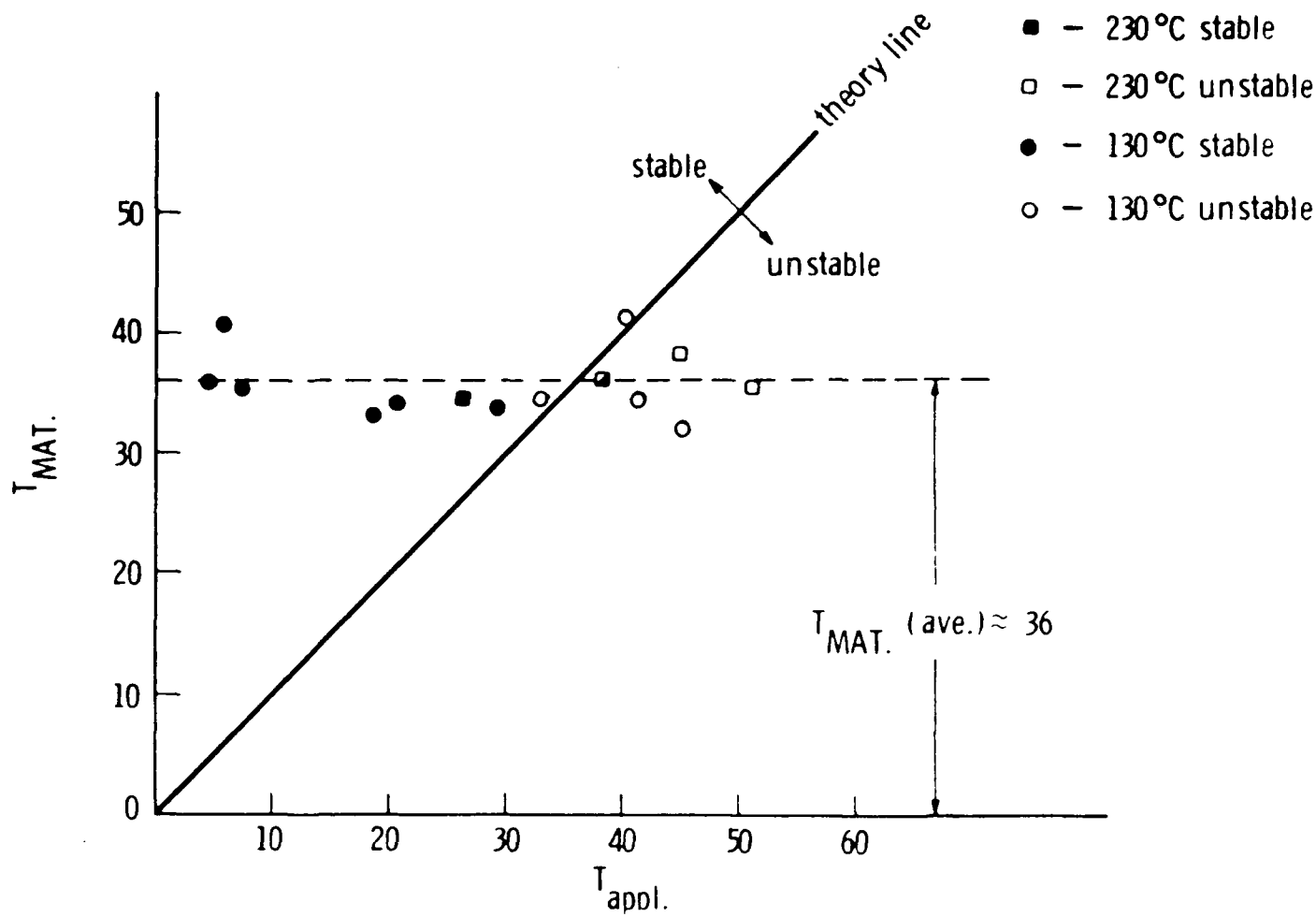

Fig. 3 –Experimental results from instability studies on a 3 point bend bar, $T_{MAT.}$ vs T_{appl}

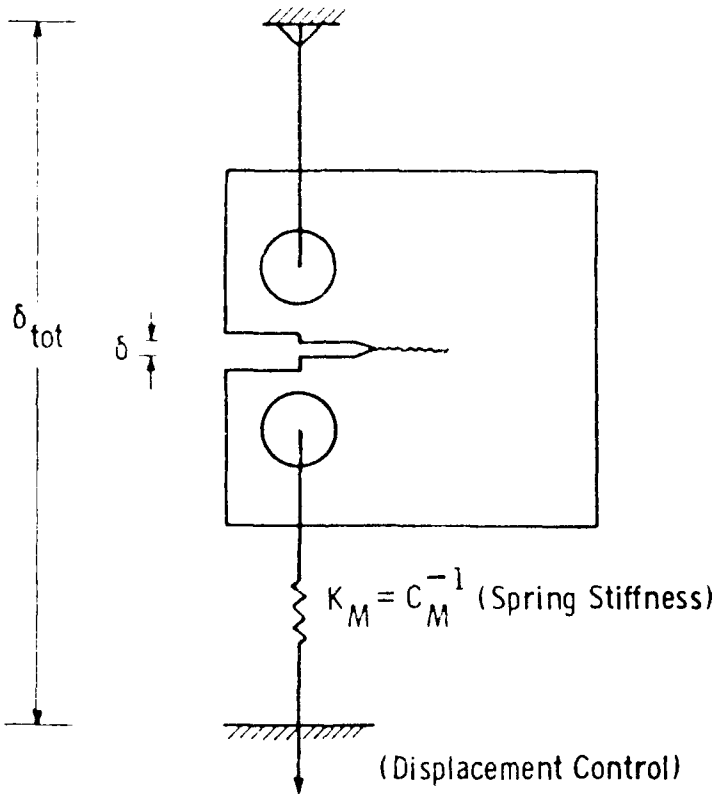

Fig. 4 — Displacement control test of a bend specimen in series with a spring bar

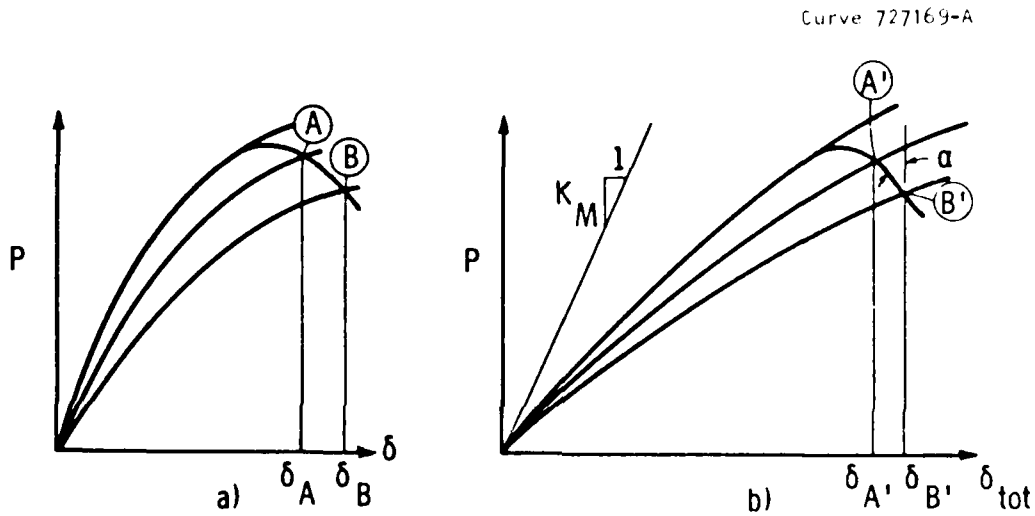

Fig. 5 — P-δ record of a specimen a) without and b) with spring in series.

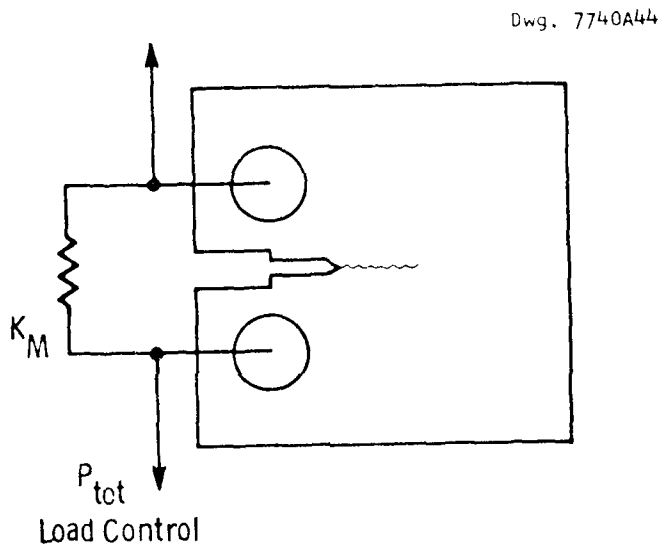

Fig. 6 — Specimen in parallel with a spring in a load-control test

Curve 728788-A

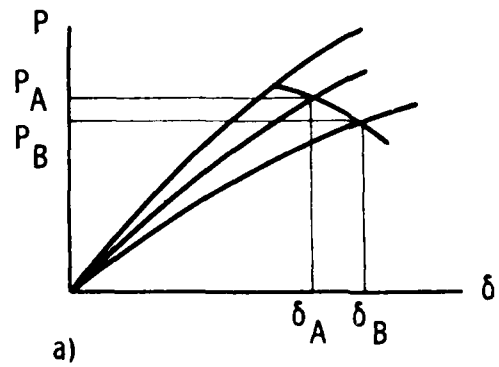

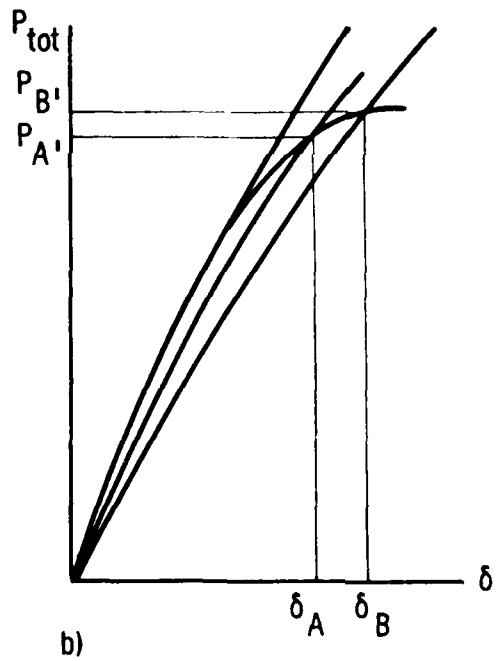

Fig. 7 — P-δ records of a specimen a) without and b) with a spring in parallel.

Curve 730515-A

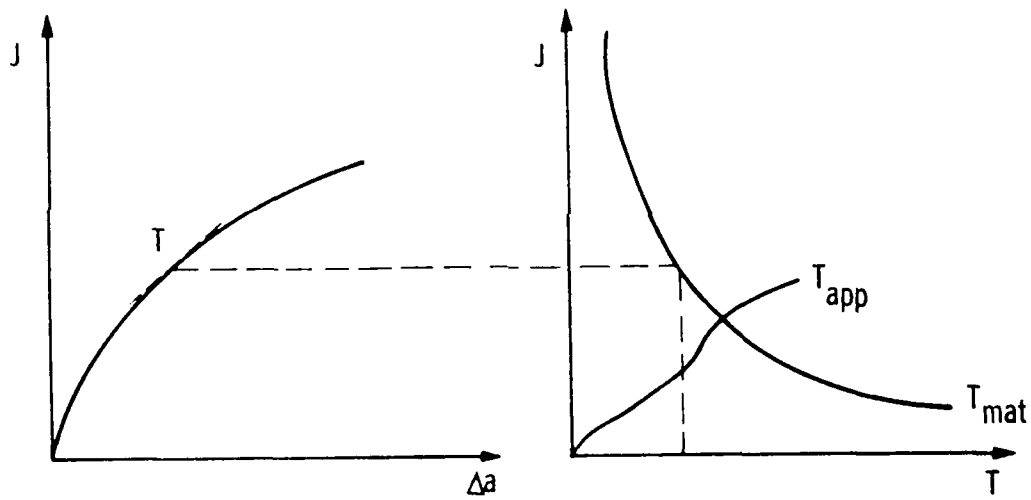

Fig. 8 – J-T plot

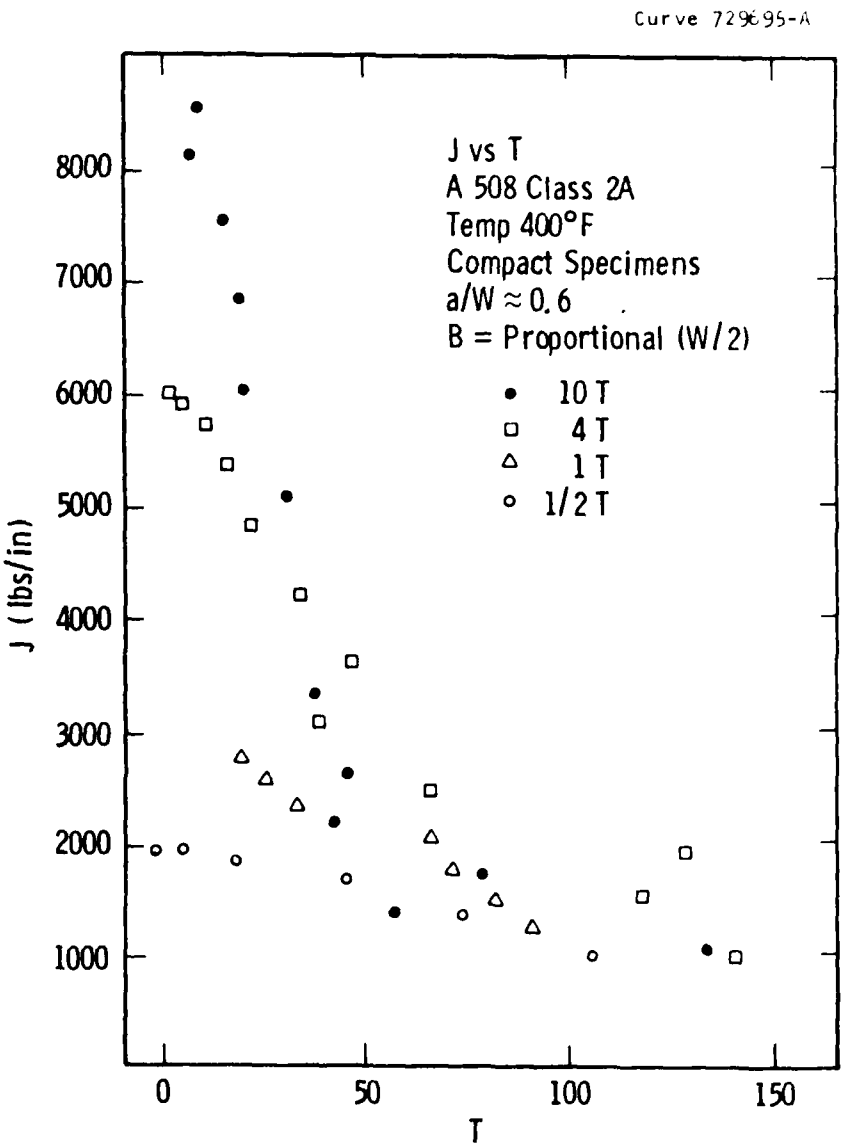
Curve 729695-A
J vs T
A 508 Class 2A
Temp 400°F
Compact Specimens
a/W ≈ 0.6
B = Proportional (W/2)
10 T
4 T
1 T
1/2 T
J (lbs/in)
8000
7000
6000
5000
4000
3000
2000
1000
0
50
100
150
T

Fig. 9 – J vs T

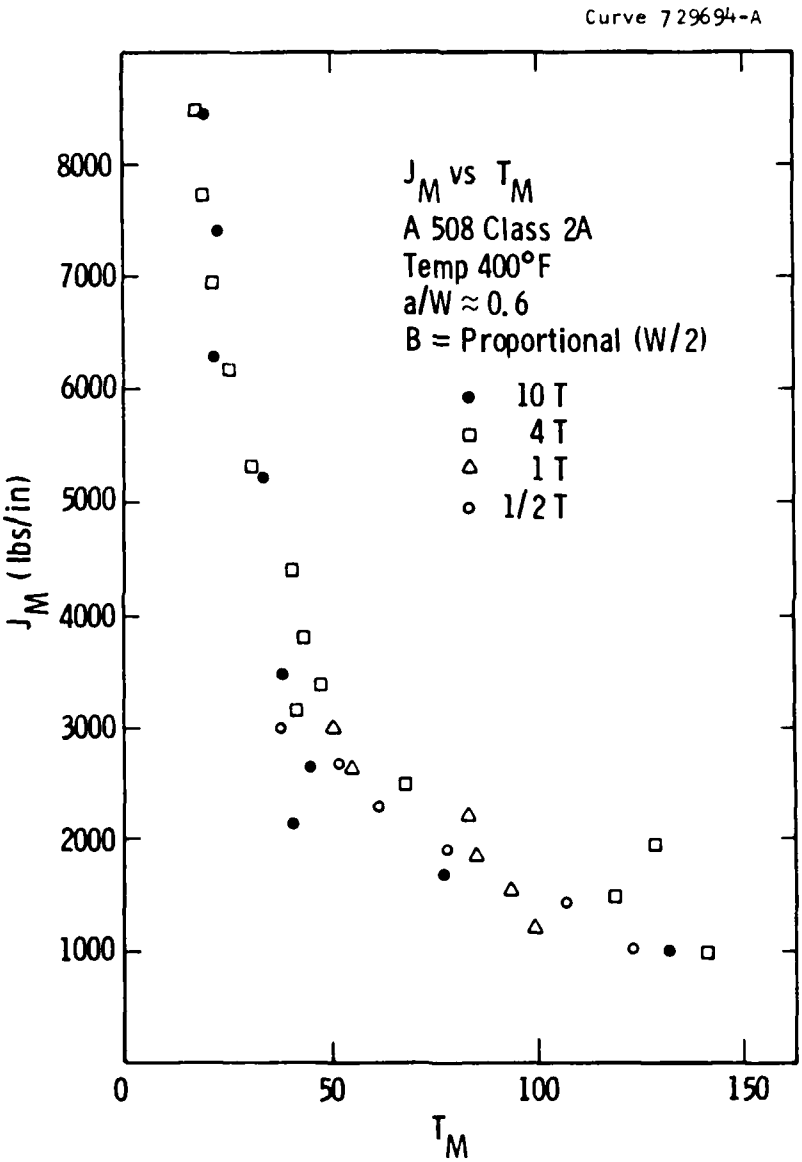

Fig. 10 – J_M vs T_M

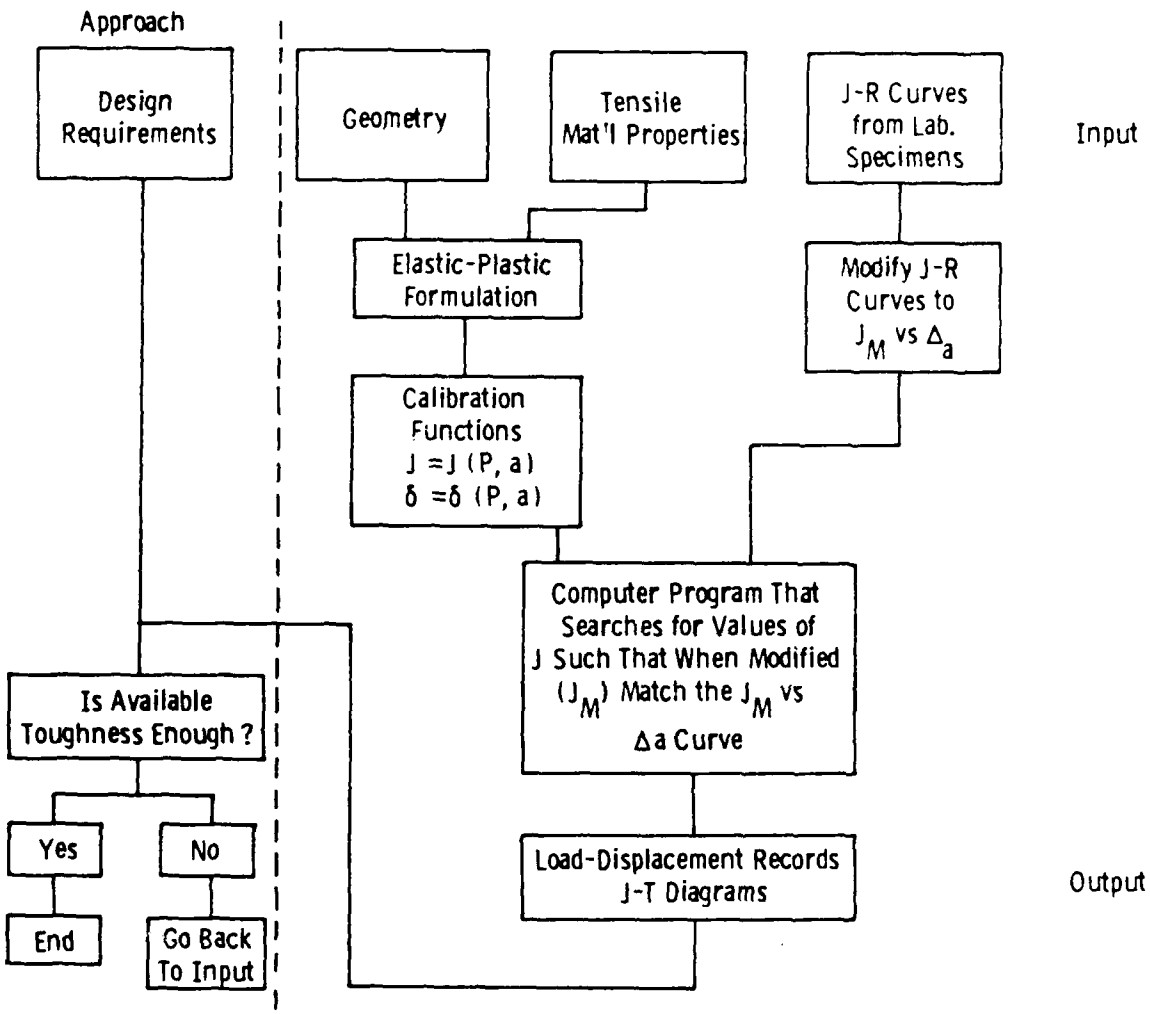

Fig. 11 – Elastic-plastic methodology

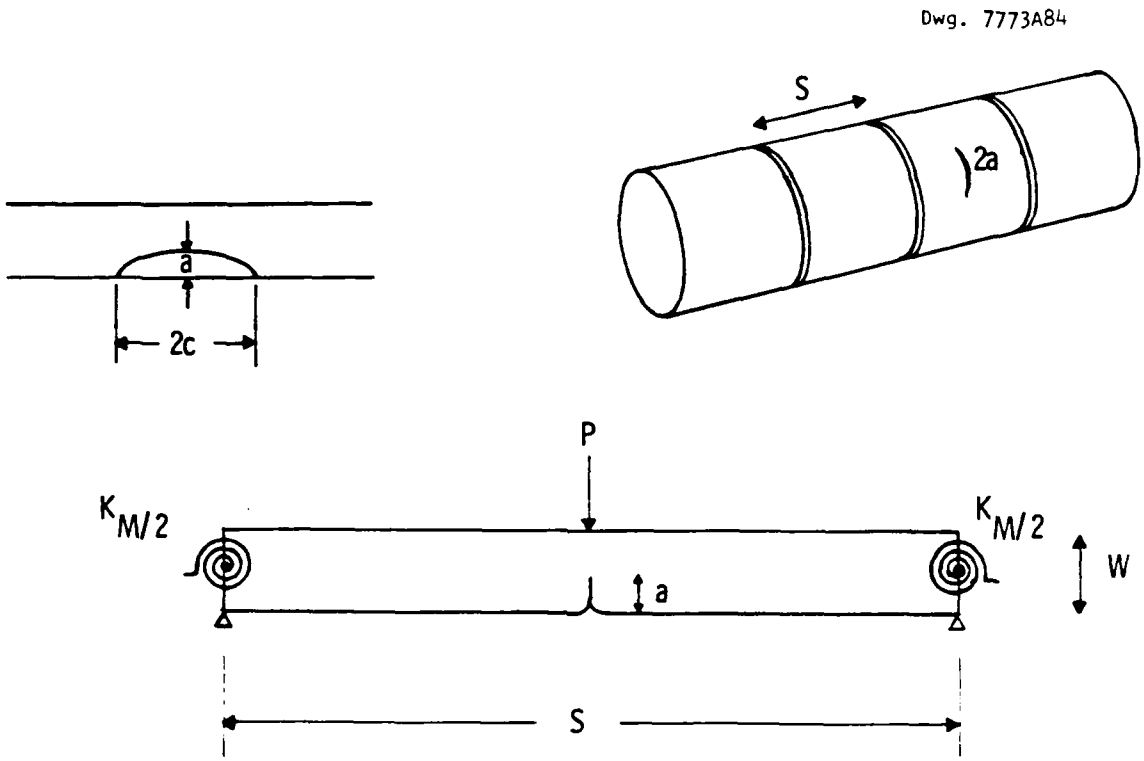

Fig. 12—Models

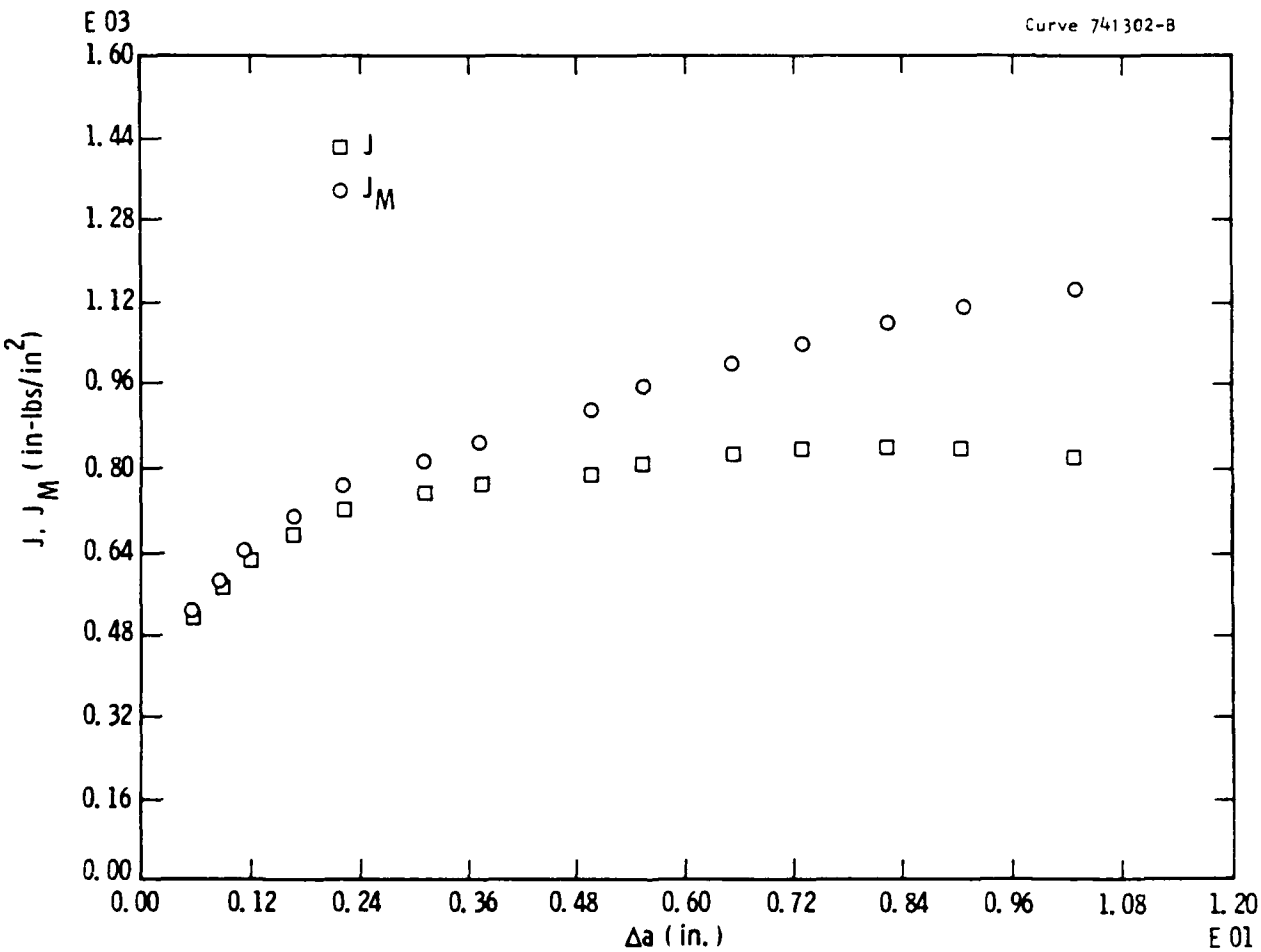

Fig. 14—J and J_M vs Δa - 1% prestrain

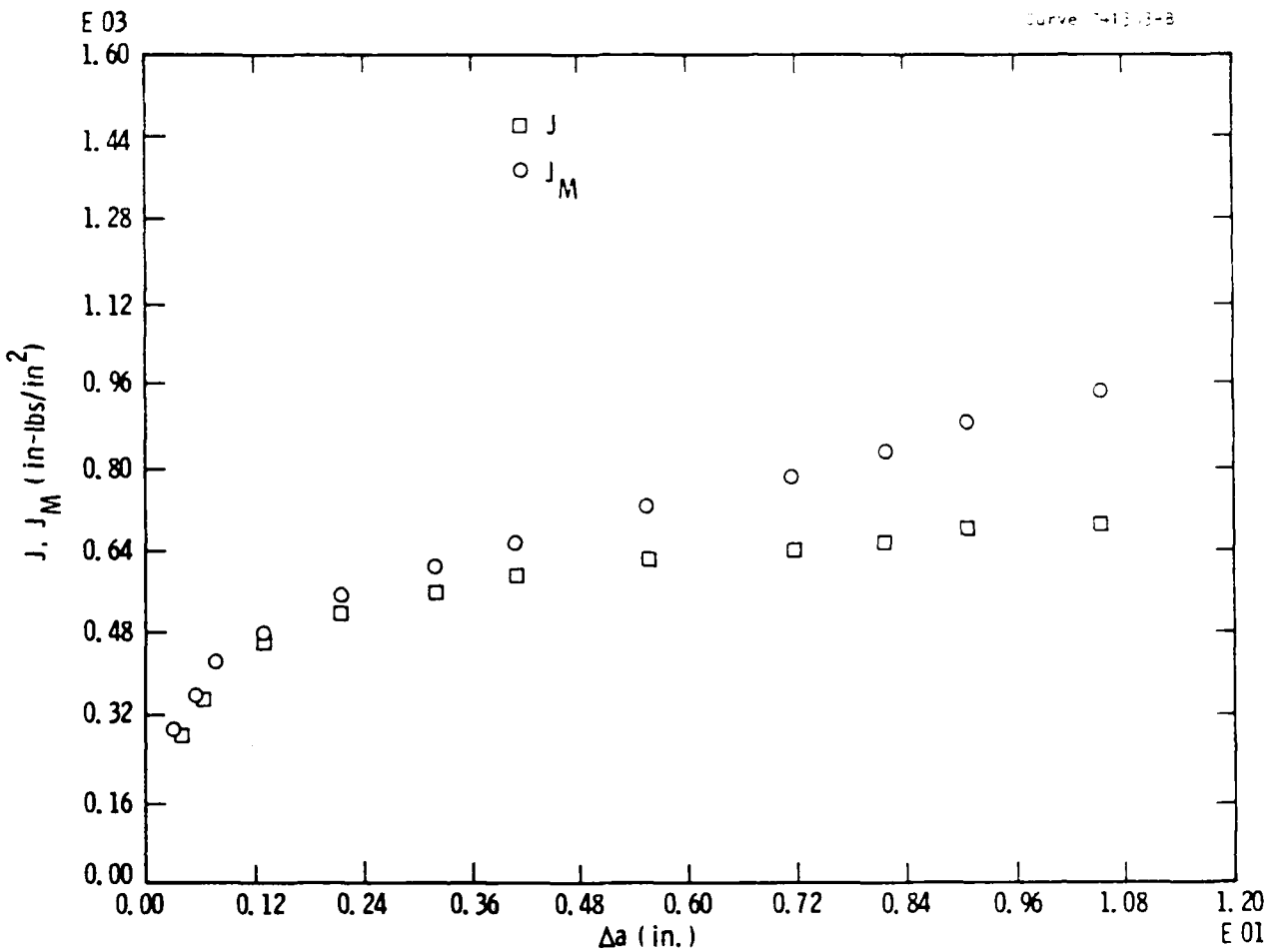

Fig. 15—J and J_M vs Δa - 3% prestrain

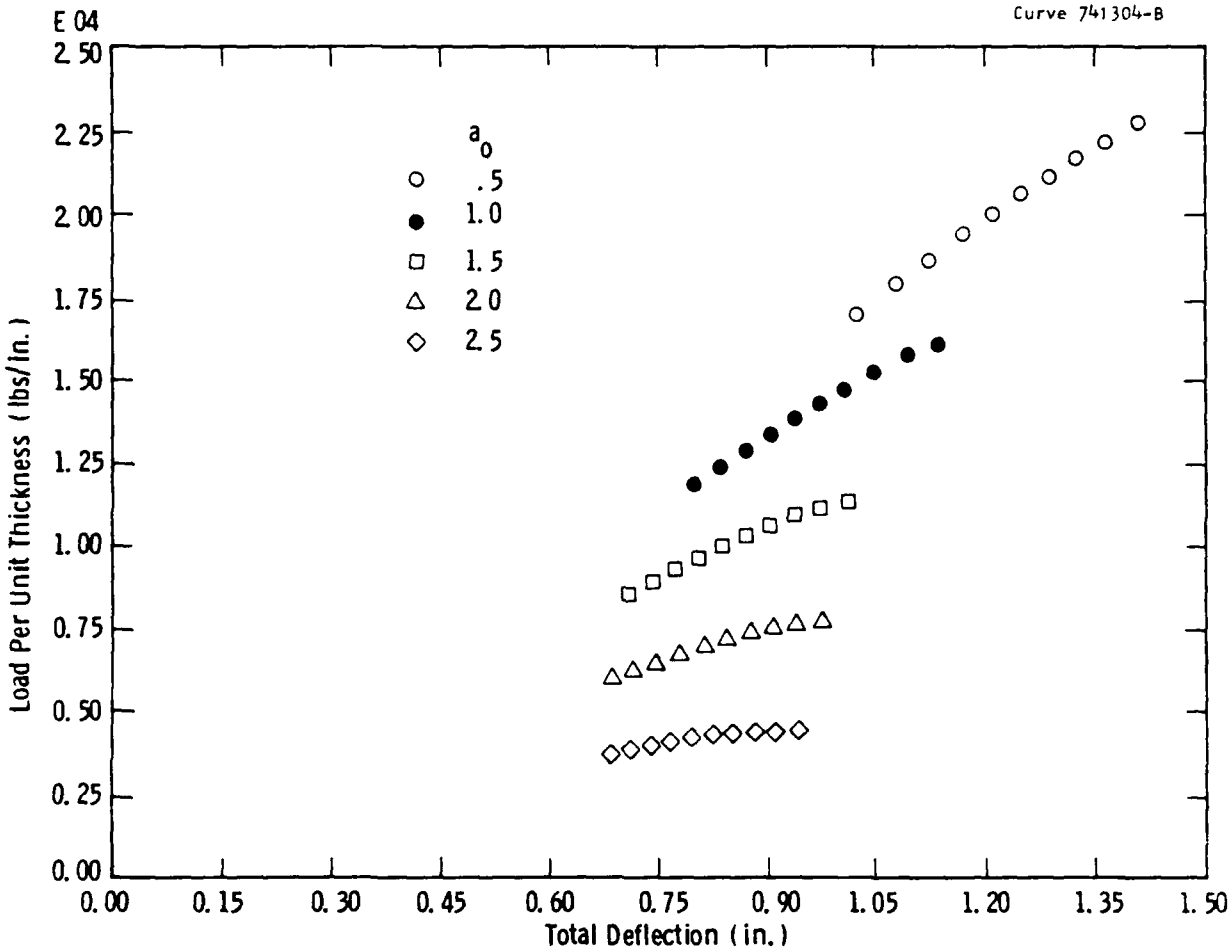

Fig. 16—Load per unit thickness vs total deflection, using J_M for different a_0 (0% prestrain)

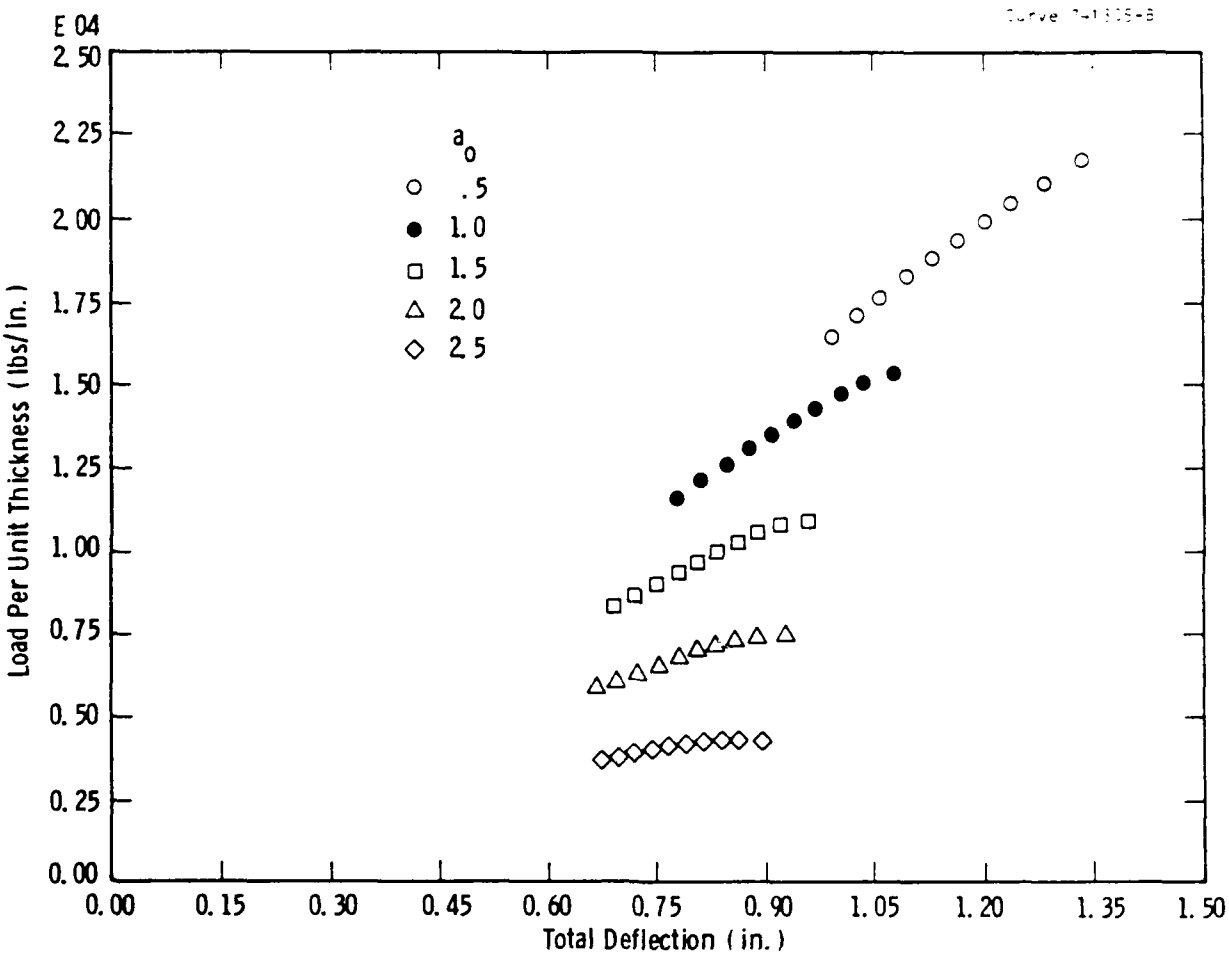

Fig. 17—Load per unit thickness vs total displacement using J_M for different a_0 (1% prestrain)

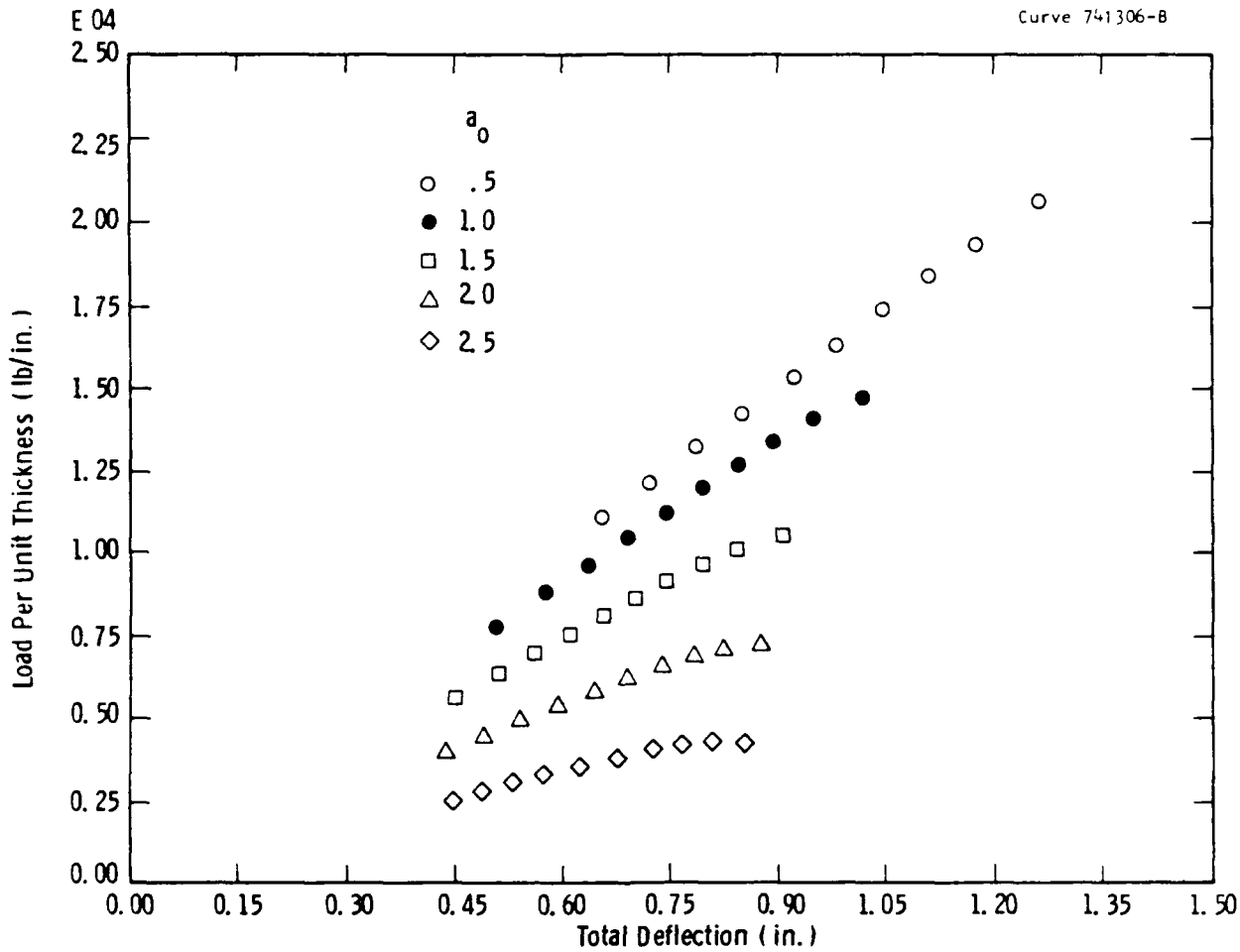

Fig. 18—Load per unit thickness vs total deflection using J_M, for different a_0 (3% prestrain)

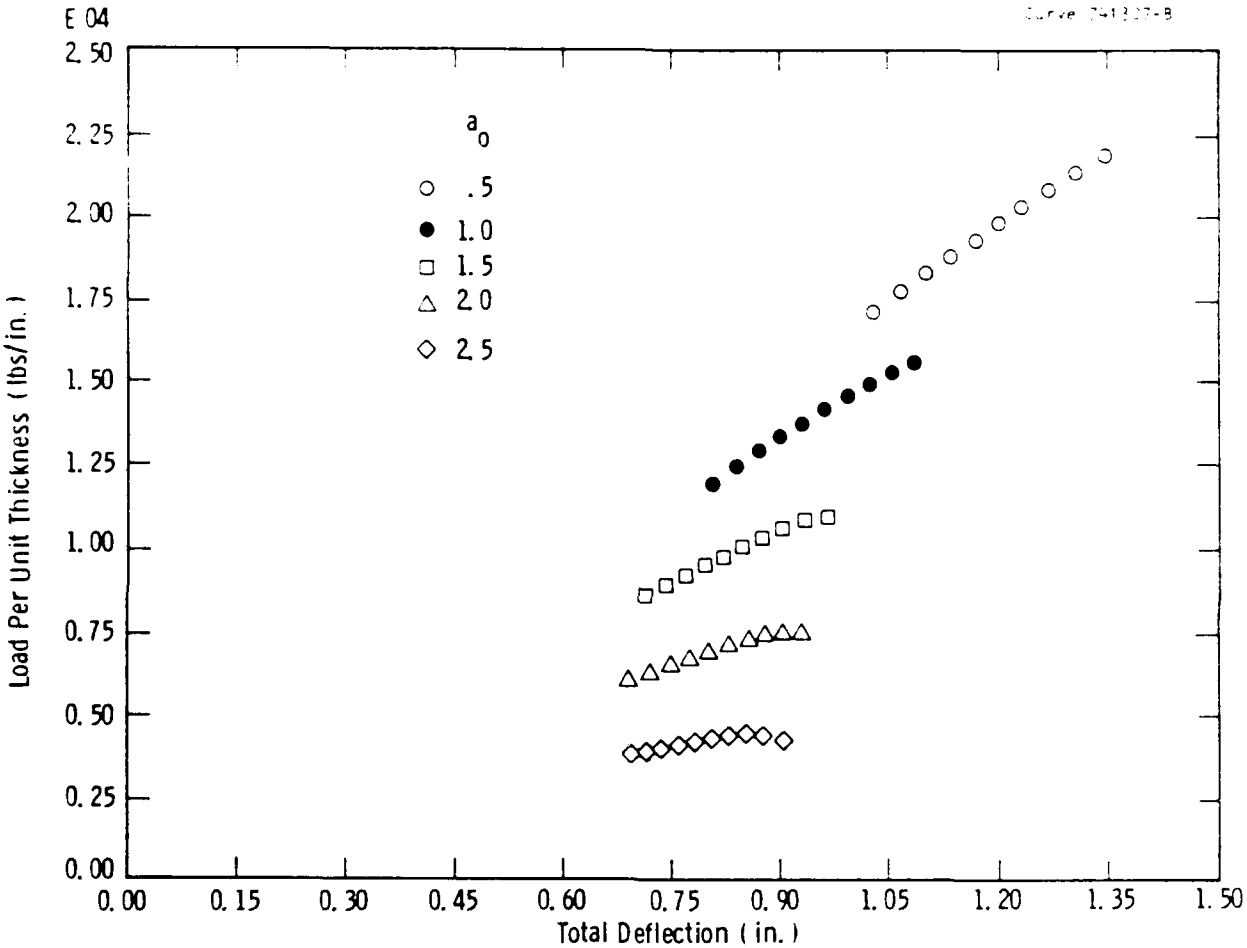

Fig. 19—Load per unit thickness vs total deflection using deformation J for different a_0 (0% prestrain)

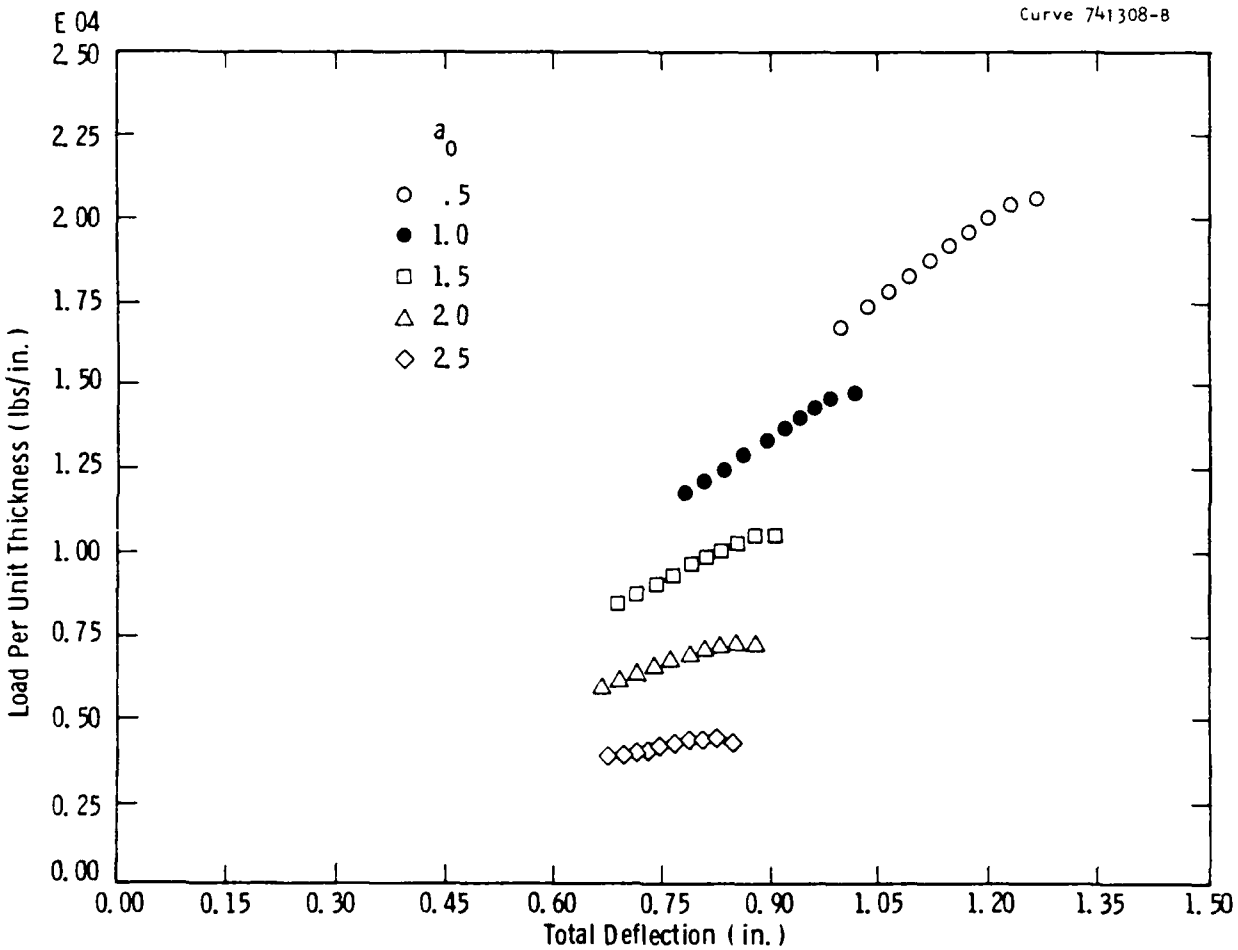

Fig. 20—Load per unit thickness vs total deflection using deformation J for different a_0 (1% prestrain)

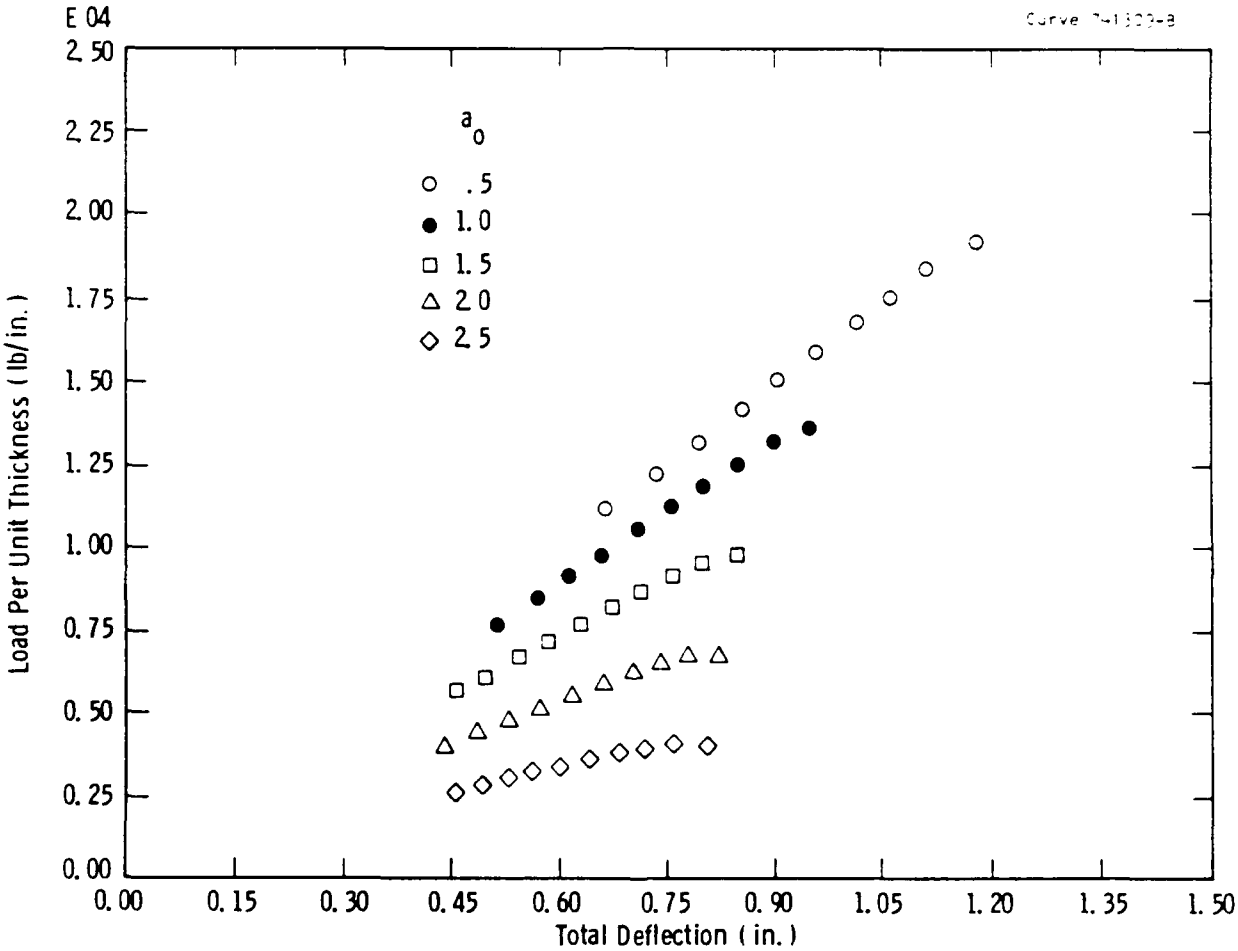

Fig. 21—Load per unit thickness vs total deflection using deformation J for different a_0 (3% prestrain)

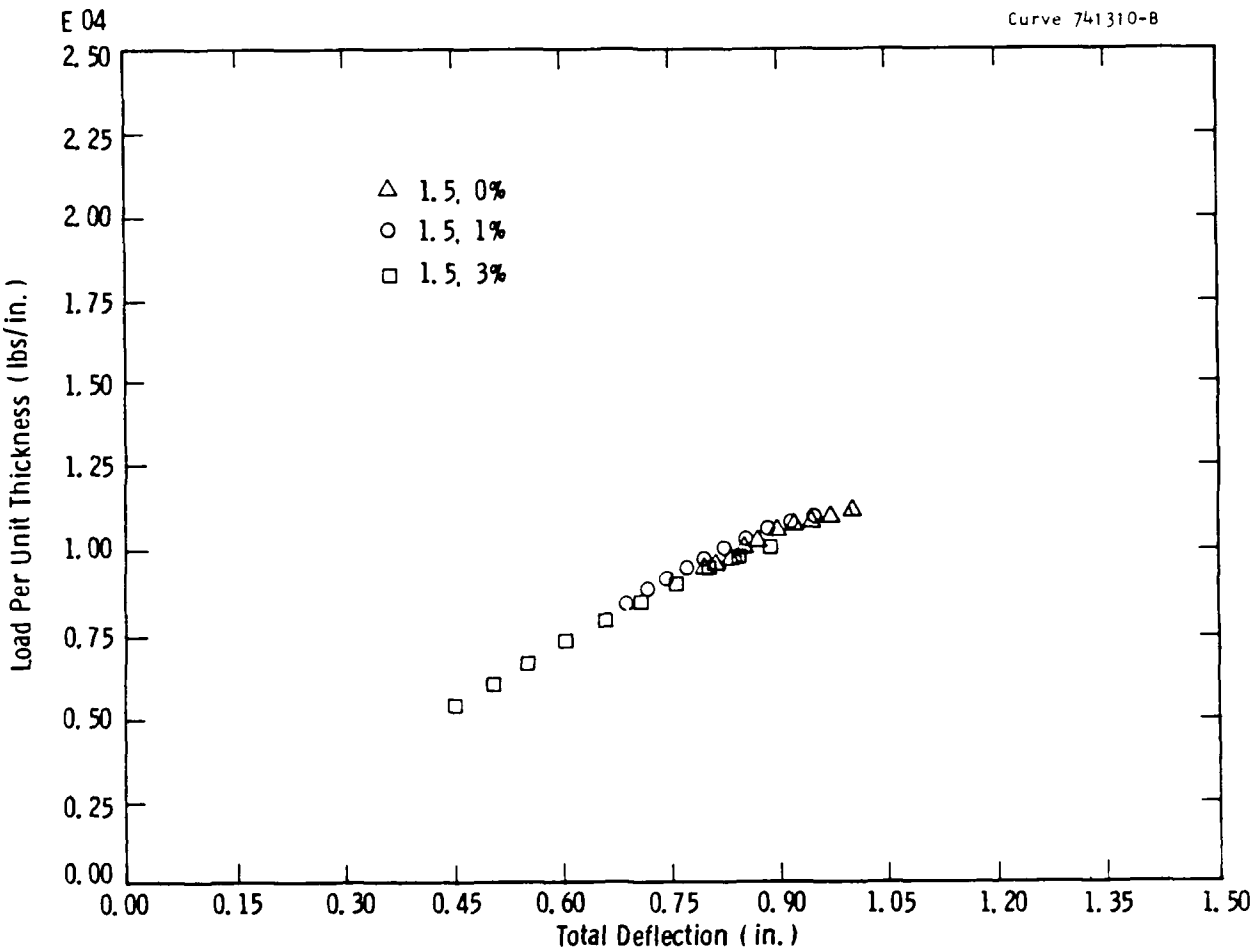

Fig. 22—Load per unit thickness vs total deflection using J_M for $a_0 = 1.5$ and different prestrain conditions

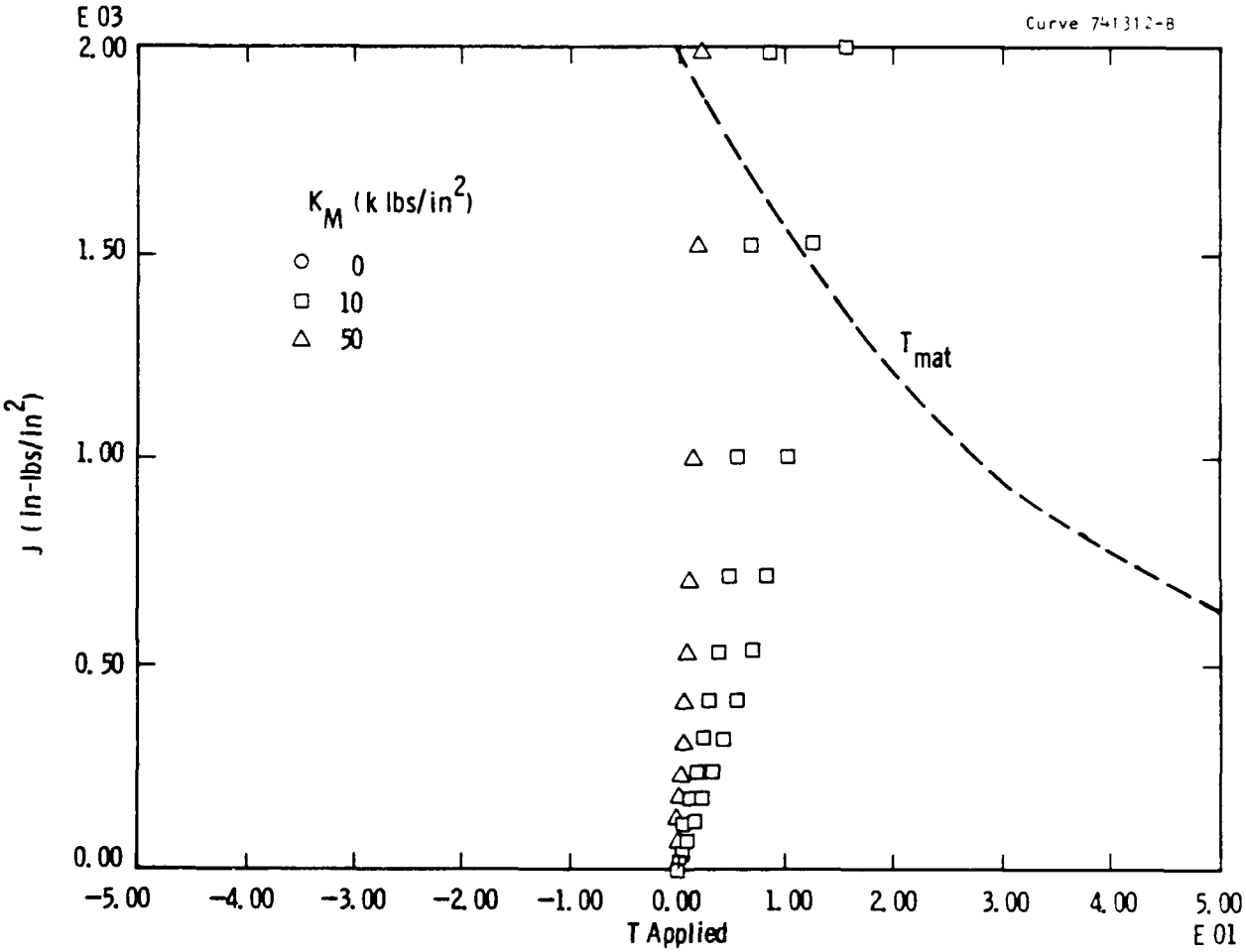

Fig. 23—J-T diagram for different spring compliances

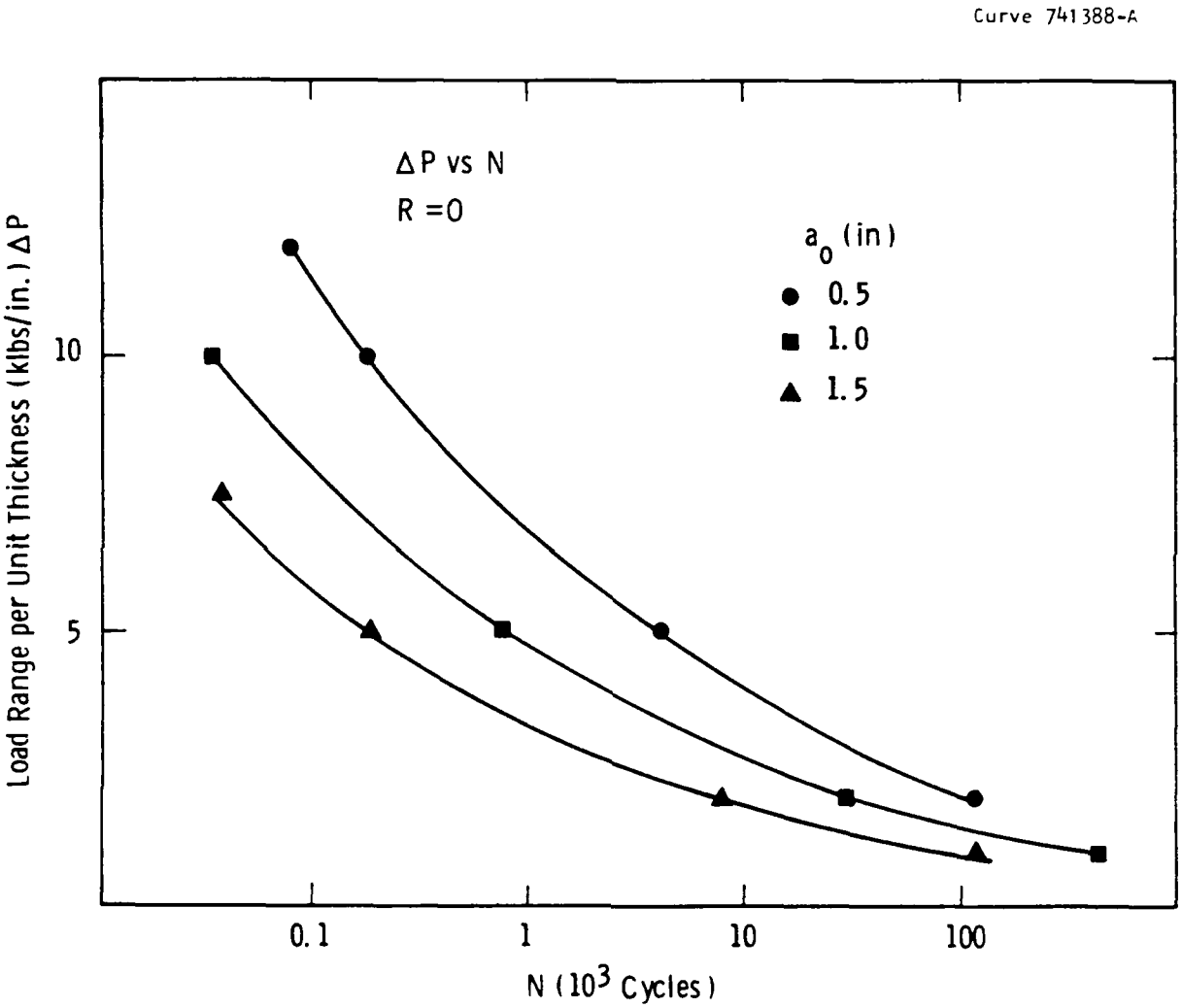

Fig. 24 – Load range (per unit thickness) vs number of cycles to failure

END

FILMED

8